Higgs bosons in a nonminimal supersymmetric model

J. Ellis*

*Stanford Linear Accelerator Center, Stanford University, Stanford, California 94305
and Lawrence Berkeley Laboratory, Berkeley, California 94720*

J. F. Gunion

Department of Physics, University of California, Davis, California 95616

H. E. Haber

Santa Cruz Institute for Particle Physics, University of California, Santa Cruz, California 95064

L. Roszkowski[†]

Department of Physics, University of California, Davis, California 95616

F. Zwirner[‡]

*Department of Physics, University of California, Berkeley, California 94720
and Lawrence Berkeley Laboratory, Berkeley, California 94720*

(Received 12 September 1988)

The minimal supersymmetric standard model contains two Higgs doublets which must mix via a mass parameter whose magnitude remains to be explained. We explore an extension of the minimal model to include a singlet Higgs field whose vacuum expectation value determines the mixing. We study the spectrum and couplings of Higgs bosons in this extended model and compare them with those in the minimal model. We examine a number of limiting cases analytically and also make numerical studies of the extended model both with and without constraints from the renormalization-group analysis of a parent superstring-inspired grand-unified-theory model. We establish the conditions for there to be a charged Higgs boson lighter than the $W^\pm$ and the circumstances under which there is no light neutral Higgs boson. With a particularly simple set of boundary conditions at the unification scale, the renormalization-group equations imply that one or more Higgs bosons are light enough to be found at the CERN LEP or SLAC Linear Collider and that many supersymmetric particles should be accessible to these accelerators and the Fermilab Tevatron; relatively few would require the Superconducting Super Collider, Large Hadron Collider, or a TeV-scale e^+e^- collider for discovery. Finally, we analyze the possible production mechanisms and phenomenological signatures of the different Higgs bosons at these machines.

I. INTRODUCTION

It is commonly agreed that the Higgs sector of the standard model is unsatisfactory because the squared mass parameter μ^2 of the minimal Higgs potential $V(H) = -\mu^2|H|^2 + \lambda(|H|^2)^2$ is not naturally of order m_W^2. Radiative corrections to μ^2 in the standard model are quadratically divergent, being $O(\alpha/\pi)\Lambda^2$ where Λ is a cutoff in the loops. Therefore, even if one could find an explanation why μ^2 was small at the tree level, one would be left with the question why radiative corrections were not much larger than the physical value of μ^2. These are the two aspects of the hierarchy problem of understanding why $m_H = \sqrt{2}\mu$ is much less than the Planck mass $m_{\rm Pl}$ and other candidates for a fundamental mass scale such as a grand-unified-theory (GUT) scale m_X.

Control of the radiative corrections so that a small value of μ^2 (and hence m_H^2 and m_W^2) becomes natural was the primary motivation of the supersymmetric standard model.[1] A light Higgs sector ($m_H^2 \ll m_{\rm Pl}^2$) is natural in a softly broken supersymmetric model since the quadratically divergent loop contributions cancel, leaving a finite correction of the form $\delta m_H^2 = O(\alpha/\pi)(m_B^2 - m_F^2)$, where $m_{B,F}$ are the masses of the bosonic and fermionic partner particles circulating in the loops. In order to give masses to all the quarks and leptons, and to cancel gauge anomalies, at least two Higgs doublets H_1, H_2 are required in a supersymmetric version of the standard model.[2] The physical spin-0 particles in the minimal supersymmetric standard model are then a complex charged Higgs boson $C^\pm$, two neutral Higgs scalars S_1, S_2, and one neutral Higgs pseudoscalar P (see Ref. 3). The properties of the Higgs bosons, including masses, mixing angles, and couplings, are determined by an effective scalar potential V which contains supersymmetric terms

$$V_0 = \sum_i |F_i|^2 + \sum_a \frac{g_a^2}{2}[D_a]^2 , \qquad (1.1)$$

where the F_i are derivatives of the superpotential W with respect to scalar fields ϕ^i: $F_i \equiv \partial W / \partial \phi^i$, and the D_a are D

terms corresponding to the different factors of the gauge group $SU(3)_C \times SU(2)_L \times U(1)_Y$, with couplings g_s, g, and g', respectively. Most expected terms in W are trilinear, but there could, in general, be a bilinear term $W \ni \mu H_1 H_2$ which would give

$$V_0 \ni \mu^2(|H_1|^2 + |H_2|^2) \qquad (1.2)$$

in obvious affinity with the squared mass term in the standard model. The effective scalar potential also contains soft supersymmetry-breaking terms of the general forms

$$V_1 = \sum_i m_i^2 |\phi^i|^2 + \left[\sum_{i,j,k} A_{ijk} \lambda_{ijk} \phi^i \phi^j \phi^k + \text{H.c.} \right], \qquad (1.3)$$

where the parameters A_{ijk} are expected to be of order m_i and phenomenology requires $|m_i| = O(m_W)$. If W contains a bilinear term $\mu H_1 H_2$, one would also expect a bilinear supersymmetry-breaking term

$$V_1 \ni B \mu H_1 H_2 + \text{H.c.} , \qquad (1.4)$$

where B is also expected to be of order m_i. This latter term is essential if the pseudoscalar P is to avoid being an unacceptable electroweak axion in the supersymmetric standard model with v_1, $v_2 \neq 0$. With a term of the form given in Eq. (1.4),

$$m_P^2 = \frac{-2B\mu}{\sin 2\beta}, \quad \tan\beta \equiv \frac{v_2}{v_1}, \quad v_i \equiv \langle 0|H_i^0|0 \rangle , \qquad (1.5)$$

and everything looks good.

Softly broken supersymmetry ensures that radiative corrections to μ are now under control so that $\mu = O(m_W) \ll m_{Pl}$ is technically natural, thus solving the easy part of the hierarchy problem. However, such a model does not provide any dynamical reason why μ should be so small in the first place. The simplest mechanism that provides a dynamical source for a term of the form Eq. (1.4) is the inclusion[4] of an additional singlet Higgs field N. Then, if the superpotential contains a trilinear term

$$W \ni \lambda N H_1 H_2 , \qquad (1.6)$$

and if N develops a vacuum expectation value $\langle N \rangle \equiv x$, a bilinear $H_1 H_2$ mixing term with

$$\mu = \lambda x \qquad (1.7)$$

is generated.[5] In the presence of soft supersymmetry breaking, one would expect $x = O(|m_i|) = O(m_W)$, and hence $\mu = O(m_W) \ll m_{Pl}$. Just such a mechanism operates in many superstring models based on E_6 (Ref. 6) and $SU(5) \times U(1)$ GUT groups[7] in which the renormalizable superpotential is purely trilinear, and automatically contains a coupling of the form (1.6) to some singlet field N.

We should mention at this point, for completeness, that alternative mechanisms for generating the term in Eq. (1.4) have been proposed.[8-10] If the vanishing of the tree-level values of μ and B is due to an exact global symmetry of the theory, then nonzero values cannot be generated by higher-order corrections. But such a symmetry

could be broken. If the breaking is spontaneous, it should occur at a scale of order 10^9–10^{12} GeV, in order for the couplings of the associated Goldstone boson to be sufficiently weak to be phenomenologically acceptable. Then, once supersymmetry is broken, radiative corrections could generate a $B\mu$ of order $(\alpha/\pi)(m_B^2 - m_F^2)$ (Ref. 8). If the breaking is explicit, a radiative generation of $B\mu$ could still occur.[9] Another mechanism,[8] operating at the tree level, would proceed via nonrenormalizable terms in the superpotential of the form $(1/m_{Pl})^{n-1}\phi^n H_1 H_2$, where ϕ is a gauge singlet acquiring a vacuum expectation value at some intermediate-mass scale $\langle \phi \rangle = M < m_{Pl}$. Yet another recent proposal[10] starts from a supergravity model whose superpotential is purely trilinear in the observable sector, but contains an explicit mass scale $M \sim 10^{10}$–10^{11} GeV in the hidden sector which breaks local supersymmetry. If the Kähler potential mixes the hidden and observable sectors in a peculiar way, then a $\mu \sim (M^2/m_{Pl}) \sim m_W$ is generated in the corresponding low-energy theory with softly broken global supersymmetry. Still, the origin of H_1-H_2 mixing presented in the previous paragraph seems to us the most appealing, and emerges in several of the phenomenologically acceptable superstring-based models.

This paper is devoted to the phenomenology of the minimal extension of the supersymmetric standard model characterized by Eqs. (1.6) and (1.7), focusing in particular on the Higgs bosons and on their couplings. The physical spectrum of the extended model contains two additional neutral Higgs bosons: one a scalar and the other a pseudoscalar. In Sec. II we discuss the general form of the effective Higgs potential and obtain the mass matrices for the charged and neutral spin-0 bosons. In Sec. III we consider various limits of the extended model, including that in which the minimal supersymmetric standard model is recovered. In Sec. IV we explore the space of model parameters consistent with the fundamental requirement of a correct gauge symmetry breaking. We emphasize that charged Higgs bosons lighter than the $W^{\pm}$ may occur in the model (in contrast with the minimal supersymmetric standard model), while the mass of the lightest neutral Higgs boson can range from a few GeV to ~ 100 GeV. In Sec. V we perform a renormalization-group analysis of the parameters in the effective low-energy potential, assuming a simple plausible pattern of supersymmetry breaking within a possible embedding in a superstring-inspired GUT, e.g., $SU(5) \times U(1)$. We discuss the resulting restrictions on the possible range of masses and parameters as allowed by the basic constraints considered in Sec. IV. In Sec. VI we analyze the couplings in the extended model, discovering that it is possible for the lightest neutral Higgs boson to have small couplings to vector bosons. In Sec. VII we discuss the phenomenological signatures of the extended model, contrasting it with the minimal supersymmetric standard model. Finally, in Sec. VIII we present some concluding remarks.

II. HIGGS POTENTIAL AND MASS MATRICES

The nonminimal supersymmetric model to be studied in the following is characterized by the superpotential

$$W = h_U Q u^c H_2 + h_D Q d^c H_1 + h_E L e^c H_1 + \lambda H_1 H_2 N$$
$$- \tfrac{1}{3} k N^3 + \cdots , \tag{2.1}$$

where gauge and generation indices are understood and the sign of the kN^3 term has been chosen for later convenience. The ellipsis stands for possible nonrenormalizable terms that can be safely neglected when considering low-energy processes if there are no intermediate mass scales between m_W and m_{Pl}, as we assume here. In comparison with the minimal supersymmetric standard model, the Higgs mixing term $W \ni \mu H_1 H_2$ has been replaced by the trilinear coupling $W \ni \lambda H_1 H_2 N$, where N is a gauge singlet. We remind the reader that the form of the superpotential is scale independent: if bilinear terms are absent at the tree level, they cannot be generated by renormalization. In this paper we focus on the minimal model of the form (2.1), namely, a model with only one "family" of Higgs bosons H_1, H_2, and N in the effective low-energy theory. We do not discuss more complicated specific superstring unification schemes[6] based on E_6 in which the singlet and doublet Higgs bosons may be replicated. Although such a replication is possible, we note the existence of superstring-inspired models [such as the flipped SU(5)×U(1) model of Ref. 7] in which there is a natural mechanism which leaves at low energy precisely two Higgs doublets and one Higgs singlet.

Supersymmetric models with the structure (2.1) have already been considered in the literature, and several potential problems have been pointed out.[8,11]

(1) If $k = 0$, the Lagrangian has a global U(1) symmetry corresponding to

$$N \rightarrow N e^{i\theta}, \quad H_1 H_2 \rightarrow H_1 H_2 e^{-i\theta} , \tag{2.2}$$

which is spontaneously broken by the vacuum expectation values (VEV's) of the Higgs fields. In order to avoid an unacceptable axion associated to this symmetry, one has to introduce into the superpotential some additional coupling [such as the $(k/3)N^3$ coupling of Eq. (2.1)] which explicitly breaks that symmetry.

(2) If the following two conditions are satisfied: (i) there are renormalizable couplings between the singlet N and superheavy chiral multiplets and (ii) supersymmetry-breaking mass splittings inside the superheavy chiral multiplets are of order $\sqrt{m_W M}$, where M is some superheavy scale, then the hierarchy $m_W \ll M$ tends to be destabilized by radiative corrections.[11] However, there is no reason to expect that both of these two conditions are satisfied. For example, in a recently proposed superstring-inspired SU(5)×U(1) model[7] condition (i) is violated. Even in models where (i) is satisfied, it might well be that inside superheavy multiplets the supersymmetry-breaking mass splittings are $O(m_W^2)$: only in the presence of a specific mechanism for supersymmetry breaking can one make a definite statement.

(3) The Lagrangian associated to the superpotential of Eq. (2.1), even after the addition of the most general soft supersymmetry-breaking terms, has a discrete $\mathbf{Z}_3$ symmetry, corresponding to a phase transformation of N of the form $N \rightarrow \alpha N$, $\alpha^3 = 1$, accompanied by suitable transformations of the remaining fields. This symmetry, if spontaneously broken in the vacuum, could create a serious cosmological domain-wall problem. However, it has been shown in Ref. 12 that a nonrenormalizable term $\sim N^4/m_{\text{Pl}}$ in Eq. (2.1) would prevent the density of domain walls from becoming large enough to cause cosmological problems, while being much too small to impact the low-energy phenomenology of the model that we focus on here.

Assuming that squark and slepton fields have vanishing vacuum expectation values, we can restrict our attention to the part of the scalar potential involving only the Higgs fields $H_1 \equiv (H_1^0, H^-)$, $H_2 \equiv (H^+, H_2^0)$, and N:

$$V_{\text{Higgs}} = V_F + V_D + V_{\text{soft}} , \tag{2.3}$$

$$V_F = |\lambda|^2 [(|H_1|^2 + |H_2|^2)|N|^2 + |H_1 H_2|^2] + |k|^2 |N|^4$$
$$- (\lambda k^* H_1 H_2 N^{*2} + \text{H.c.})$$
$$- |\lambda|^2 (H_1^0 H_2^0 H^{+*} H^{-*} + \text{H.c.}) , \tag{2.4}$$

$$V_D = \frac{g^2}{8}(H_2^\dagger \sigma H_2 + H_1^\dagger \sigma H_1)^2 + \frac{g'^2}{8}(|H_2|^2 - |H_1|^2)^2 , \tag{2.5}$$

$$V_{\text{soft}} = m_{H_1}^2 |H_1|^2 + m_{H_2}^2 |H_2|^2 + m_N^2 |N|^2$$
$$- (\lambda A_\lambda H_1 H_2 N + \text{H.c.}) - (\tfrac{1}{3} k A_k N^3 + \text{H.c.}) . \tag{2.6}$$

The absence of an explicit soft supersymmetry-breaking term of the form given in Eq. (1.4) is a natural assumption. If such a term is absent at the grand unification scale then the renormalization-group equations[13] imply that such a term is not generated in evolving down to the low-energy scale. To fix unambiguously the notation, $H_1 H_2 \equiv H_1^0 H_2^0 - H^- H^+$, $\sigma \equiv (\sigma^1, \sigma^2, \sigma^3)$ are the Pauli matrices, and asterisks denote complex conjugation. In general λ, k, A_λ, and A_k can be complex numbers. Redefining conveniently the global phase of the fields H_2 and N one can always assume, without loss of generality,

$$\lambda A_\lambda \in \mathbf{R}^+, \quad k A_k \in \mathbf{R}^+ . \tag{2.7}$$

Moreover, the requirement of no explicit CP violation in the scalar sector gives

$$\lambda k^* \in \mathbf{R} . \tag{2.8}$$

In the real world, we know that CP-violating observables are small, so the assumption (2.8) may not require large corrections. A simple solution to (2.7) and (2.8), which will be assumed in the following, is to take $\lambda, k, A_\lambda, A_k \in \mathbf{R}$. Making an SU(2)$_L$ ×U(1)$_Y$ gauge transformation, it is not restrictive to assume

$$v^+ \equiv \langle H^+ \rangle = 0, \quad v_2 \equiv \langle H_2^0 \rangle \in \mathbf{R}^+ . \tag{2.9}$$

One can then write

$$\langle V_{\text{Higgs}} \rangle = \langle V_{\text{neutral}} \rangle + \langle V_{\text{charged}} \rangle , \tag{2.10}$$

where

$$\langle V_{\text{neutral}} \rangle = \lambda^2 (|x|^2 |v_1|^2 + |x|^2 v_2^2 + |v_1|^2 v_2^2) + k^2 |x|^4 - \lambda k v_2 (v_1^* x^2 + v_1 x^{2*})$$

$$+ \frac{g^2 + g'^2}{8} (|v_1|^2 - v_2^2)^2 + m_{H_1}^2 |v_1|^2 + m_{H_2}^2 v_2^2 + m_N^2 |x|^2 - \lambda A_\lambda v_2 (v_1 x + v_1^* x^*) - \frac{k A_k}{3} (x^3 + x^{*3}) \qquad (2.11)$$

and

$$\langle V_{\text{charged}} \rangle = |v^-|^2 \left[m_{H_2}^2 + \lambda^2 |x|^2 + \frac{g^2}{4} (|v_1|^2 + v_2^2) \right.$$

$$\left. + \frac{g'^2}{4} (|v_1|^2 - v_2^2) \right]$$

$$+ \frac{g^2 + g'^2}{8} |v^-|^4 . \qquad (2.12)$$

We now analyze the potential of Eqs. (2.11) and (2.12). Note that, in contrast with the minimal case, in the present model one has to check for the absence of charge-breaking minima with $v^- \neq 0$. The condition for $v^- = 0$ to be a *local* minimum is

$$m_{H_2}^2 + \lambda^2 |x|^2 + \frac{g^2}{4} (|v_1|^2 + v_2^2) + \frac{g'^2}{4} (|v_1|^2 - v_2^2) > 0 , \qquad (2.13)$$

which is equivalent to the requirement that the physical charged Higgs bosons of the model have positive mass squared. It will be straightforward to delineate the parameter constraints required in order that this be true. However, we will see later that condition (2.13) does not always guarantee that $v^- = 0$ corresponds to a *global* minimum. Next, we note that the presence of three different terms in $\langle V_{\text{neutral}} \rangle$ which depend on the phase of the VEV's v_1 and x allows in principle for spontaneous *CP* violation. A sufficient condition for the vacuum to conserve *CP* is

$$\lambda k \in \mathbf{R}^+ , \qquad (2.14)$$

which we assume hereafter. If (2.14) holds, the minimization condition on the phases of v_1 and x gives rise to three equivalent vacua. Defining $x \equiv \rho_0 e^{i\phi_0}, v_1 = \rho_1 e^{\phi_1}$, for $\rho_0, \rho_1 \in \mathbf{R}^+$ they are given by

$$\phi_0 = 0, \quad \phi_1 = 0 ,$$

$$\phi_0 = \frac{2\pi}{3}, \quad \phi_1 = \frac{4\pi}{3} , \qquad (2.15)$$

$$\phi_0 = \frac{4\pi}{3}, \quad \phi_1 = \frac{2\pi}{3} .$$

We will work in the first of these vacua: as noted above, the degeneracy between them can be broken without impacting the low-energy physics we study here.

For values of the parameters such that the minimum of V_{Higgs} corresponds to $v_1, v_2, x > 0$, one can use the minimization conditions to reexpress the soft supersymmetry-breaking masses $m_{H_1}^2, m_{H_2}^2, m_N^2$ in terms of the three VEV's and of the remaining parameters $\lambda, k, A_\lambda, A_k$:

$$m_{H_1}^2 = \lambda A_\lambda \frac{v_2 x}{v_1} - \lambda^2 (x^2 + v_2^2) + \lambda k \frac{v_2 x^2}{v_1}$$

$$+ \frac{g^2 + g'^2}{4} (v_2^2 - v_1^2) ,$$

$$m_{H_2}^2 = \lambda A_\lambda \frac{v_1 x}{v_2} - \lambda^2 (x^2 + v_1^2) + \lambda k \frac{v_1 x^2}{v_2}$$

$$+ \frac{g^2 + g'^2}{4} (v_1^2 - v_2^2) , \qquad (2.16)$$

$$m_N^2 = \lambda A_\lambda \frac{v_1 v_2}{x} + k A_k x - \lambda^2 (v_1^2 + v_2^2) - 2k^2 x^2$$

$$+ 2\lambda k v_1 v_2 .$$

Taking into account the constraint $m_W^2 = \frac{1}{2} g^2 (v_1^2 + v_2^2)$, one can then express the mass terms for the Higgs fields in terms of the six parameters $\lambda, k, A_\lambda, A_k, x$, and $\tan\beta$.

The physical charged Higgs field is given by

$$C^+ \equiv \cos\beta H^+ + \sin\beta H^{-*} , \qquad (2.17)$$

while the orthogonal combination corresponds to an unphysical Goldstone boson. The squared mass of the charged boson (2.17) is given by

$$m_C^2 = m_W^2 - \lambda^2 (v_1^2 + v_2^2) + \lambda (A_\lambda + kx) \frac{2x}{\sin 2\beta} , \qquad (2.18)$$

which may be less or greater than m_W^2, depending upon the relative sizes of the last two terms. [Note that the last term must be positive definite as a result of Eqs. (2.7) and (2.14).] Because of their frequent occurrences, it will be convenient to define

$$A_\Sigma \equiv A_\lambda + kx \qquad (2.19)$$

as well as

$$v \equiv (v_1^2 + v_2^2)^{1/2} , \qquad (2.20)$$

$$r \equiv \frac{x}{v} , \qquad (2.21)$$

and also

$$\bar{g} \equiv \frac{1}{\sqrt{2}} \sqrt{g^2 + g'^2} . \qquad (2.22)$$

Decomposing the neutral Higgs fields into their real and imaginary components

$$H_1^0 \equiv \frac{H_{1R}^0 + iH_{1I}^0}{\sqrt{2}} ,$$

$$H_2^0 \equiv \frac{H_{2R}^0 + iH_{2I}^0}{\sqrt{2}} , \qquad (2.23)$$

$$N \equiv \frac{N_R + iN_I}{\sqrt{2}} ,$$

the corresponding mass matrices decouple. After expressing H_{1I}^0 and H_{2I}^0 in terms of the neutral Goldstone boson $G^0 \equiv \cos\beta H_{1I}^0 - \sin\beta H_{2I}^0$ and of the orthogonal combination of fields $A^0 \equiv \sin\beta H_{1I}^0 + \cos\beta H_{2I}^0$, the squared mass matrix for the two physical "pseudoscalar" neutral Higgs fields reads

$$\mathcal{M}_P^2 = \begin{bmatrix} \lambda A_\Sigma \dfrac{xv^2}{v_1 v_2} & \lambda v(A_\Sigma - 3kx) \\[2ex] \lambda v(A_\Sigma - 3kx) & \lambda A_\Sigma \dfrac{v_1 v_2}{x} + 3k A_k x + 3\lambda k v_1 v_2 \end{bmatrix}$$

(2.24)

and the solution of its eigenvalue problem is a matter of elementary algebra. We first note that the resulting eigenvalues $m_{P_1}^2$ and $m_{P_2}^2$ are guaranteed to be positive. This is because both the determinant and the trace of $\mathcal{M}_P^2$ are positive given Eqs. (2.7) and (2.14). It is most useful to write the results in terms of the entries in

$$\mathcal{M}_P^2 \equiv \begin{bmatrix} R & S \\ S & T \end{bmatrix}.$$

Let us define the matrix U^P to be that which transforms from the A^0-N_I basis to the diagonal mass basis P_1-P_2: i.e.,

$$\begin{bmatrix} P_1 \\ P_2 \end{bmatrix} = U^P \begin{bmatrix} A^0 \\ N_I \end{bmatrix}.$$

(2.25)

Writing

$$U^P \equiv \begin{bmatrix} \cos\gamma & \sin\gamma \\ -\sin\gamma & \cos\gamma \end{bmatrix}$$

(2.26)

we find

$$\sin 2\gamma = \frac{-2S}{\sqrt{(T-R)^2 + 4S^2}},$$

$$\cos 2\gamma = \frac{T-R}{\sqrt{(T-R)^2 + 4S^2}},$$

(2.27)

and eigenvalues

$$m_{P_1,P_2}^2 = \tfrac{1}{2}[(T+R) \mp \sqrt{(T-R)^2 + 4S^2}],$$

(2.28)

where

$$T \pm R = \frac{\lambda A_\Sigma v_1 v_2}{x} + 3k(xA_k + \lambda v_1 v_2) \pm \frac{\lambda A_\Sigma xv^2}{v_1 v_2},$$

$$S = \lambda v(A_\Sigma - 3kx).$$

(2.29)

The angle γ may be chosen between 0 and π according to

$$\gamma \in \begin{cases} \left[0, \dfrac{\pi}{4}\right], & S < 0, \quad T > R, \\[2ex] \left[\dfrac{\pi}{4}, \dfrac{\pi}{2}\right], & S < 0, \quad T < R, \\[2ex] \left[\dfrac{\pi}{2}, \dfrac{3\pi}{4}\right], & S > 0, \quad T < R, \\[2ex] \left[\dfrac{3\pi}{4}, \pi\right], & S > 0, \quad T > R. \end{cases}$$

(2.30)

In terms of the original H_{1I}-H_{2I}-N_I basis, the two physical pseudoscalar states are given as

$$P_1 = \begin{bmatrix} \cos\gamma \sin\beta \\ \cos\gamma \cos\beta \\ \sin\gamma \end{bmatrix}, \quad P_2 = \begin{bmatrix} -\sin\gamma \sin\beta \\ -\sin\gamma \cos\beta \\ \cos\gamma \end{bmatrix}.$$

(2.31)

Limiting cases of the pseudoscalar states are considered in Sec. III, and exact numerical results in Sec. IV.

The squared mass matrix for the "scalar" neutral Higgs fields H_{1R}^0, H_{2R}^0, and N_R takes the form

$$\lambda \begin{bmatrix} \dfrac{\bar{g}^2 v_1^2}{\lambda} + \dfrac{A_\Sigma x v_2}{v_1} & -A_\Sigma x + \dfrac{v_1 v_2}{\lambda}(2\lambda^2 - \bar{g}^2) & v_2\left[\dfrac{2\lambda v_1 x}{v_2} - kx - A_\Sigma\right] \\[2ex] -A_\Sigma x + \dfrac{v_1 v_2}{\lambda}(2\lambda^2 - \bar{g}^2) & \dfrac{\bar{g}^2 v_2^2}{\lambda} + \dfrac{A_\Sigma x v_1}{v_2} & v_1\left[\dfrac{2\lambda v_2 x}{v_1} - kx - A_\Sigma\right] \\[2ex] v_2\left[\dfrac{2\lambda v_1 x}{v_2} - kx - A_\Sigma\right] & v_1\left[\dfrac{2\lambda v_2 x}{v_1} - kx - A_\Sigma\right] & \dfrac{4k^2 x^2 - k A_k x}{\lambda} + \dfrac{A_\lambda v_1 v_2}{x} \end{bmatrix}.$$

(2.32)

It is not useful to present analytic results for the diagonalization of this matrix. We refer the reader to Sec. III for certain limiting cases and to Sec. IV for numerical results.

As a general point of notation, for both the pseudoscalar and the scalar Higgs bosons, the components of the eigenvectors in the H_1^0-H_2^0-N basis will be denoted by $\mathcal{P}_\alpha^i$

and $\mathcal{S}_a^i$, respectively, where $i = 1,2,3$ indicates H_1^0, H_2^0, N, $\alpha = 1,2$ denotes P_1, P_2, and $a = 1,2,3$ denotes S_1, S_2, S_3, the mass eigenstates of Eq. (2.32). It should be noted that we label the S_a and P_α in order of increasing mass. It will also be convenient to define a two-component charged Higgs eigenvector

$$\mathcal{C}_+ \equiv \mathcal{C}_- \equiv \begin{bmatrix} \sin\beta \\ \cos\beta \end{bmatrix} , \qquad (2.33)$$

so that $\mathcal{C}_+^l$, $l = 1,2$ denotes the two components given above. Finally, we define the matrix U^S as

$$U^S = \begin{bmatrix} \mathcal{S}_1^1 & \mathcal{S}_1^2 & \mathcal{S}_1^3 \\ \mathcal{S}_2^1 & \mathcal{S}_2^2 & \mathcal{S}_2^3 \\ \mathcal{S}_3^1 & \mathcal{S}_3^2 & \mathcal{S}_3^3 \end{bmatrix} . \qquad (2.34)$$

Since we are assuming that the Higgs sector conserves CP, U^S is a real orthogonal matrix. Thus, for instance,

$$\begin{bmatrix} \mathrm{Re}H_1^0 \\ \mathrm{Re}H_2^0 \\ \mathrm{Re}N \end{bmatrix} = \begin{bmatrix} v_1 \\ v_2 \\ x \end{bmatrix} + \frac{1}{\sqrt{2}}(U^S)^T \begin{bmatrix} S_1 \\ S_2 \\ S_3 \end{bmatrix} , \qquad (2.35)$$

or in component form

$$\mathrm{Re}H_1^0 = v_1 + \frac{1}{\sqrt{2}}(\mathcal{S}_1^1 S_1 + \mathcal{S}_2^1 S_2 + \mathcal{S}_3^1 S_3) ,$$

$$\mathrm{Re}H_2^0 = v_2 + \frac{1}{\sqrt{2}}(\mathcal{S}_1^2 S_1 + \mathcal{S}_2^2 S_2 + \mathcal{S}_3^2 S_3) , \qquad (2.36)$$

$$\mathrm{Re}N = x + \frac{1}{\sqrt{2}}(\mathcal{S}_1^3 S_1 + \mathcal{S}_2^3 S_2 + \mathcal{S}_3^3 S_3) .$$

This eigenvector notation will be useful in specifying the couplings of the Higgs bosons to other particles and among themselves.

III. SPECIAL LIMITING CASES

The specific predictions of the model described in the previous section depend on the physical mass eigenstates of the Higgs-pseudoscalar and -scalar mass matrices. The pseudoscalar mass matrix is 2×2 and can be easily diagonalized; the corresponding masses and eigenstates have been given in Eqs. (2.28) and (2.31). The scalar mass matrix is 3×3, so no simple analytic expressions for the masses and the eigenstates can be obtained. Nevertheless, there are various limiting cases in which the Higgs-scalar masses and mixing angles can be evaluated perturbatively. In this section, we examine three limiting cases: (i) $x \gg v_1, v_2$, with λ and k fixed, (ii) $x \gg v_1, v_2$, with λx and kx fixed (and nonzero), and (iii) $x \ll v_1$ and v_2. Case (ii) is of interest, since in this limit the minimal supersymmetric model with two Higgs doublets and no Higgs singlets is obtained. This allows us to examine the nature of the deviations from the minimal supersymmetric model, due to the singlet Higgs field. It should be emphasized that not all of these limits may be numerically relevant to models which emerge from renormalization-group analyses. Moreover, unlike the case of E_6-based models,[6] where x is related to the mass of a new Z' gauge boson and is therefore likely to be larger than v_1 and v_2, the parameter x in our model is not so constrained, and small values of x as in our case (iii) become possible. The analytic results obtained in this section are useful for two reasons. First, they provide a guide to the behavior of the system in general and, second, they provide checks on the numerical analysis which we later perform.

A. Limit of $x \gg v_1, v_2$ (λ, k fixed)

We may diagonalize the scalar mass matrix [Eq. (2.32)] perturbatively in the parameters v_1/x and v_2/x. In the formulas we present below, we shall assume that A_Σ is of $O(x)$. In particular, our formulas break down if A_λ increases faster than x as x gets large. Among the three scalar mass eigenstates, S_1, S_2, and S_3, we find that S_1 and S_2 are dominantly H_1 and H_2 (with $m_{S_1} < m_{S_2}$) and S_3 is dominantly N, in the large-x limit. In this limit, the tree-level (squared) masses are

$$m_{S_1}^2 = m_Z^2 \cos^2 2\beta$$
$$+ \lambda^2 v^2 \left\{ \sin^2 2\beta - \frac{1}{k^2}[\lambda - \tfrac{1}{2}(k + A_\Sigma/x)\sin 2\beta]^2 \right\} , \qquad (3.1)$$

$$m_{S_2}^2 = \frac{2\lambda x A_\Sigma}{\sin 2\beta} + (m_Z^2 - \lambda^2 v^2)\sin^2 2\beta$$
$$- \frac{\lambda^2 v^2 (k + A_\Sigma/x)^2 \cos^2 2\beta}{4k^2 - \dfrac{2\lambda A_\Sigma}{x \sin 2\beta}} , \qquad (3.2)$$

$$m_{S_3}^2 = 4k^2 x^2 - k A_k x + \frac{\lambda^2 v^2}{k^2}[\lambda - \tfrac{1}{2}(k + A_\Sigma/x)\sin 2\beta]^2$$
$$+ \frac{\lambda^2 v^2 (k + A_\Sigma/x)^2 \cos^2 2\beta}{4k^2 - \dfrac{2\lambda A_\Sigma}{x \sin 2\beta}} . \qquad (3.3)$$

The corresponding mass eigenstates, in this approximation, are conveniently summarized by the matrix U^S [see Eq. (2.34)]:

$$U^S = \begin{bmatrix} \cos\beta & \sin\beta & \dfrac{-\lambda v}{4k^2 x}[2\lambda - (k + A_\Sigma/x)\sin 2\beta] \\[2ex] -\sin\beta & \cos\beta & \dfrac{-\lambda v}{2kx}\dfrac{(k + A_\Sigma/x)\cos 2\beta}{\dfrac{\lambda}{\sin 2\beta} - 2k} \\[3ex] U_{31}^S & U_{32}^S & 1 \end{bmatrix} , \qquad (3.4)$$

where

$$U_{31}^S = \frac{\lambda v}{2kx} \left| \frac{[2\lambda - (k + A_\Sigma/x)\sin 2\beta]\cos\beta}{2k} \right.$$
$$\left. - \frac{(k + A_\Sigma/x)\cos 2\beta \sin\beta}{\dfrac{\lambda}{\sin 2\beta} - 2k} \right| , \qquad (3.5)$$

$$U_{32}^S = \frac{\lambda v}{2kx}\left[\frac{[2\lambda-(k+A_\Sigma/x)\sin2\beta]\sin\beta}{2k} \right.$$

$$\left. + \frac{(k+A_\Sigma/x)\cos2\beta\cos\beta}{\dfrac{\lambda}{\sin2\beta}-2k} \right], \qquad (3.6)$$

and terms of $O(1/x^2)$ have been dropped. Note that these forms imply that S_3 is mainly $\mathrm{Re}N-x$ at large x.

Results for the Higgs-pseudoscalar masses are

$$m_{P_1}^2 = 3kxA_k, \qquad m_{P_2}^2 = \frac{2\lambda x A_\Sigma}{\sin2\beta} \qquad (3.7)$$

and the mixing angle γ of Eq. (2.27) has the limit $\gamma \to \pi/2$, implying that P_1 is mainly $\mathrm{Im}N$, while P_2 is a mixture of $\mathrm{Im}H_1^0$ and $\mathrm{Im}H_2^0$. Thus, like S_3, P_1 tends to decouple from nonsinglet matter fields. This decoupling for these two Higgs bosons implies that they would be essentially impossible to produce or detect in the large-x limit.

By examining the above equations, we may make a number of useful remarks. First, we note that $m_{S_1}^2$ is not obviously positive. This imposes a certain constraint on the parameters of the model, in order that the vacuum be stable. To give an example, suppose that $v_1 = v_2$ (so that $\cos2\beta = 0$). Then $m_{S_1}^2 \geq 0$ implies

$$k \geq \left| k + \frac{A_\lambda}{2x} - \lambda \right| \quad \text{for } v_1 = v_2 . \qquad (3.8)$$

If A_λ is of $O(x)$ then we deduce that $A_\lambda \leq 2x\lambda$. This in turn imposes an upper bound on the value of the charged-Higgs-boson mass:

$$m_C^2 \lesssim 2\lambda x^2(k+2\lambda) \quad \text{for } v_1 = v_2 \qquad (3.9)$$

(where we have displayed only the leading term in x). For $v_1 \neq v_2$, the expressions become much more complicated but similar conclusions can be drawn.

A second condition can be derived by requiring that $m_{S_3}^2 \geq 0$. To leading order in x, we obtain $A_k \leq 4kx$. Note that in the limit of large x, all other scalar and pseudoscalar mass squares are positive. However, even if the symmetry-breaking vacuum is stable, we must check that it is a deeper minimum than the symmetric vacuum. This condition imposes a second independent requirement on our parameters. The general condition works out to be

$$\lambda^2 v^2 x^2 + (\lambda v_1 v_2 - kx^2)^2 \geq \lambda A v_1 v_2 x + \tfrac{1}{3}k A_k x^3$$

$$+ \tfrac{1}{2}m_Z^2 v^2 \cos^2 2\beta . \qquad (3.10)$$

In the limit of large x, this second condition reduces to $A_k \leq 3kx$, which is a slightly stronger requirement than the one previously obtained.

Next, we examine relations among the Higgs-boson masses imposed by supersymmetry. First, we recall mass relations which have been obtained in other supersymmetric extensions of the standard model.[1] In the minimal supersymmetric model, there is no singlet Higgs field N.

In this minimal model, two parameters—$\tan\beta$ and one Higgs-boson mass—are sufficient to fix the remaining Higgs-boson masses and scalar Higgs mixing angle. The Higgs-boson mass relations in the minimal model are

$$m_C^2 = m_P^2 + m_W^2 , \qquad (3.11)$$

$$m_{S_1,S_2}^2 = \tfrac{1}{2}(m_P^2+m_Z^2 \mp [(m_P^2+m_Z^2)^2$$

$$-4m_Z^2 m_P^2\cos^2 2\beta]^{1/2}) . \qquad (3.12)$$

By convention, we take $m_{S_1} \leq m_{S_2}$. Furthermore, there is only one pseudoscalar in the minimal model, which we denote by P. The above relations imply that the Higgs-boson masses are restricted such that (i) $m_{S_1} \leq m_P$, (ii) $m_{S_1} \leq m_Z|\cos2\beta| \leq m_Z$, (iii) $m_{S_2} \geq m_Z$, and (iv) $m_C \geq m_W$. Furthermore, Eq. (3.12) implies the sum rule

$$m_{S_1}^2 + m_{S_2}^2 = m_P^2 + m_Z^2 . \qquad (3.13)$$

E_6-based models, in which the "low-energy" electroweak group is larger than $\mathrm{SU}(2)_L \times \mathrm{U}(1)_Y$, inevitably contain extra $\mathrm{SU}(2)_L \times \mathrm{U}(1)_Y$-singlet Higgs scalars.[6,14,15] Note that the latter transform nontrivially under E_6, unlike the N field in our model which is a singlet under the full gauge group. In models with an extra low-energy $\mathrm{U}(1)$, Eq. (3.11) is typically violated in the following fashion:

$$m_C^2 = m_P^2 + m_W^2 - \lambda^2 v^2 + O\left[\frac{m_Z}{m_{Z'}}\right] , \qquad (3.14)$$

where Z' is the new gauge boson resulting from the extra $\mathrm{U}(1)$ and is presumed to be heavier than the Z. On the other hand, the sum rule given in Eq. (3.13), when appropriately generalized, remains true:[14]

$$\mathrm{Tr}\mathcal{M}_S^2 = \mathrm{Tr}\mathcal{M}_Z^2 + \mathrm{Tr}\mathcal{M}_P^2 , \qquad (3.15)$$

where the traces are taken over the scalar, pseudoscalar, and the neutral-vector-boson mass matrices of the extended model.

We now investigate the extent of the sum-rule violations in the nonminimal model described in Sec. II. Using the exact forms for the pseudoscalar and charged-Higgs-boson masses given in Eqs. (2.24) and (2.32), we can write

$$m_C^2 = \mathrm{Tr}\mathcal{M}_P^2 + m_W^2 - \lambda^2 v^2 - \lambda A_\Sigma \frac{v_1 v_2}{x}$$

$$-3k(\lambda v_1 v_2 + A_k x) . \qquad (3.16)$$

Even if we drop terms of $O(1/x)$, we see that Eq. (3.11) is violated. The extent of the violation bears some resemblance to Eq. (3.14), but there are important differences. First, there is no Z' in our model, which means that the large-x limit need not be the relevant one. Second, even if we substitute the trace of the pseudoscalar mass matrix for m_P, corrections to Eq. (3.14) in our model are of $O(x)$. Nevertheless, such corrections are still small compared to $\mathrm{Tr}\mathcal{M}_P^2$ which is of $O(x^2)$ in the large-x limit. The conclusion in our case is clear: the charged Higgs boson can be lighter than the W, unlike the case of the

minimal model, where it is strictly heavier than the W.

Second, in our model (unlike the E_6-based models), the neutral-boson sum rule [Eq. (3.15)] is violated:

$$\text{Tr}\mathcal{M}_S^2 = m_Z^2 + \text{Tr}\mathcal{M}_P^2 + 4k(kx^2 - A_k x - \lambda v_1 v_2) . \quad (3.17)$$

Not surprisingly, the sum-rule violation is entirely due to the parameter k. Furthermore, there is no upper limit to the mass of the lightest scalar Higgs boson. In contrast with the minimal model, where S_1 is necessarily lighter than the Z, we see that in the present case, m_{S_1} can be arbitrarily large, as long as

$$\sin 2\beta > \frac{2\lambda}{3k + A_\Sigma/x} . \quad (3.18)$$

If this condition holds, then $m_{S_1}^2$ increases without bound as λ^2 increases. Of course, in order for the latter to be consistent with Eq. (3.18), k must also increase at least as fast as λ. Although this behavior is mathematically possible, it is clear that any perturbative analysis will break down if λ or k are too large. Furthermore, the condition of perturbative unification restricts the size of λ and k to be no larger than ~ 1, as we shall see in Sec. V. Such a condition would therefore lead to an upper bound for m_{S_1} of $O(m_Z)$.

B. Limit of $x \gg v_1, v_2$ ($\lambda x, kx$ fixed)

We have noted above that the sum rules of the minimal model are violated in any model which contains a gauge-singlet Higgs field. We can only restore the sum rules of the minimal model by taking the limit of our theory in which $x \to \infty$, $\lambda, k \to 0$, with λx, kx, A_k, and A_λ held fixed (in which limit A_Σ is also fixed). As in the previous large-x case, S_1 and S_2 decouple from S_3, and P_1 and P_2 decouple from one another, with S_3 approaching $\text{Re}N - x$. The two pseudoscalars have masses as given in Eq. (3.7). However, unlike the previous large-x limit with λ, k fixed, both these masses remain finite (as does m_{S_3}) when λx and kx are held fixed as $x \to \infty$. Which mass corresponds to P_1 and which to P_2, depends on the relative magnitude of the two masses (which is not fixed in this limit). However, it is always the Higgs pseudoscalar with mass $3kx A_k$ which approaches $\text{Im}N$. For the purpose of discussion, let us assume that it is this pseudoscalar which is the *heavier* of the two. By our naming conventions, we must then call this pseudoscalar P_2 (Ref. 16). In this case, the angle γ defined in Eq. (2.26) has the limit $\gamma \to 0$. Then, the S_3 and P_2 would be impossible to produce or detect at accelerators in the limit being considered. It is easy to verify that in this limit, S_1, S_2, and P_1 satisfy all the equations [Eq. (3.11) and (3.12)] of the minimal model; i.e., the sum rules are restored. In addition, we may compute the S_1-S_2 mixing angle α in this limit:

$$\sin 2\alpha = \frac{-(1+y)\sin 2\beta}{\sqrt{1+y^2 - 2y \cos 4\beta}} , \quad (3.19)$$

where

$$y = \frac{2\lambda A_\Sigma x}{m_Z^2 \sin 2\beta} . \quad (3.20)$$

(Here, we employ the notation of Ref. 3, where $-\pi/2 \leq \alpha \leq 0$.) By choosing λx and kx appropriately, we can arrange for any value of α we please (subject to the restriction just noted). Thus, this particular limit is indeed precisely equivalent to the minimal model. If a low-energy Higgs sector were to be observed, it would be important to check for deviations from the sum rules predicted by the minimal supersymmetric model. It is interesting to note that although the sum-rule violation [see Eq. (3.17)] was proportional to k, the deviation from the sum rule exhibited by the subset of particles S_1, S_2, and P_1 is proportional to λ^2. The reason for this is that for $\lambda = 0$ the latter set of Higgs fields decouples exactly from S_3 and P_2 and the sum rule is then precisely obeyed.

C. Limit of $x \ll v_1, v_2$

The limit of small x is perhaps more interesting in that it seems closer to the typical result which emerges from the renormalization-group analysis (see Sec. V). We now exhibit the Higgs-boson masses, keeping terms through $O(x)$. The tree-level (squared) masses are

$$m_{S_1}^2 = \tfrac{1}{2} m_Z^2 \left[1 - \frac{\cos 2\beta}{\cos 2\alpha} \right] + 2\lambda A_\lambda x \sin 2\alpha , \quad (3.21)$$

$$m_{S_2}^2 = \tfrac{1}{2} m_Z^2 \left[1 + \frac{\cos 2\beta}{\cos 2\alpha} \right] - 2\lambda A_\lambda x \sin 2\alpha , \quad (3.22)$$

$$m_{S_3}^2 = \frac{\lambda A_\lambda v^2 \sin 2\beta}{2x} + \frac{2\lambda A_\lambda x}{\sin 2\beta} - k A_k x , \quad (3.23)$$

where α is the S_1-S_2 mixing angle in the limit where $x = 0$. Explicitly,

$$\sin 2\alpha = \frac{(2\lambda^2 v^2 - m_Z^2)\sin 2\beta}{[m_Z^4 \cos^2 2\beta + (2\lambda^2 v^2 - m_Z^2)^2 \sin^2 2\beta]^{1/2}} , \quad (3.24)$$

$$\cos 2\alpha = \frac{m_Z^2 \cos 2\beta}{[m_Z^4 \cos^2 2\beta + (2\lambda^2 v^2 - m_Z^2)^2 \sin^2 2\beta]^{1/2}} . \quad (3.25)$$

Note that unlike in the large-x limit, the sign of α can be positive or negative (i.e., we may take $-\pi/2 \leq \alpha \leq \pi/2$). The corresponding eigenstates can be read off from the mixing matrix U^S given below:

$$U^S = \begin{bmatrix} -\sin\alpha + C\cos\alpha & \cos\alpha + C\sin\alpha & \dfrac{-2x\sin\beta}{v\sin 2\beta} \\[2ex] \cos\alpha + C\sin\alpha & \sin\alpha - C\cos\alpha & \dfrac{-2x\cos\beta}{v\sin 2\beta} \\[2ex] \dfrac{2x\cos(\alpha+\beta)}{v\sin 2\beta} & \dfrac{2x\sin(\alpha+\beta)}{v\sin 2\beta} & 1 \end{bmatrix} , \quad (3.26)$$

where we have defined C to be

$$C \equiv \frac{2\lambda A_\lambda x \cos 2\alpha \sin[2(\beta - \alpha)]}{m_Z^2 \sin 4\beta} . \quad (3.27)$$

It is also useful to give the pseudoscalar masses in the small-x limit:

$$m_{P_1}^2 = \frac{18\lambda k x^2}{\sin 2\beta} + O(x^3) \ , \tag{3.28}$$

$$m_{P_2}^2 = \frac{\lambda A_\lambda v^2 \sin 2\beta}{2x} + 2\lambda k v^2 \sin 2\beta + \frac{2\lambda A_\lambda x}{\sin 2\beta} + 3k A_k x$$

$$+ O(x^2) \ . \tag{3.29}$$

Note that as $x \to 0$, $m_{P_2}^2 \simeq m_{S_3}^2$.

Regarding the field content of the Higgs-boson mass eigenstates, it is important to note that in this small-x limit, $S_3 \to \mathrm{Re}N - x$ and $P_2 \to \mathrm{Im}N$. Thus, in this limit S_3 and P_2 decouple from ordinary matter and will not be easily produced or detected. This is clearly analogous to the situation found in the large x, fixed λ, k limit, except that there it was the lighter pseudoscalar P_1 that decoupled.

If we check the mass sum rules as before, keeping only the Higgs bosons S_1, S_2, and P_1, then the correct result through $O(x)$ is $\mathrm{Tr}\mathcal{M}_S^2 = m_Z^2$. Thus, unlike in the case of the minimal model, we find here that *two* scalars are lighter than the Z. [Curiously, if we define the trace to sum over all scalars and pseudoscalars, *including* the S_3 and P_2 states whose masses are growing like $1/x$, we find

$$\mathrm{Tr}\mathcal{M}_S^2 = m_Z^2 + \mathrm{Tr}\mathcal{M}_P^2 - 4k A_k x \ , \tag{3.30}$$

which approaches the sum rule of Eq. (3.15) as $x \to 0$.] The charged-Higgs-boson mass satisfies

$$m_C^2 = m_W^2 - \lambda^2 v^2 + \frac{2\lambda A_\lambda x}{\sin 2\beta} \ . \tag{3.31}$$

Thus for small x, the charged Higgs boson is strictly lighter than the W, so long as large values of A_λ are not considered. (In any case, our small-x expansion breaks down if A_λ is too large.) Alternatively, one can use Eq. (3.31) to set an upper bound on λ at a given value of A_λ and x:

$$\lambda^2 v^2 \le m_W^2 + \frac{2 A_\lambda x m_W}{v \sin 2\beta} \ . \tag{3.32}$$

We can get more detailed bounds on the light scalar masses by examining Eqs. (3.21) and (3.22). We find

$$m_{S_1}^2 \le \tfrac{1}{2} m_Z^2 + \frac{\sqrt{2} m_Z A_\lambda x}{v} \ , \tag{3.33}$$

$$\tfrac{1}{2} m_Z^2 - \frac{\sqrt{2} m_Z A_\lambda x}{v} \le m_{S_2}^2 \le \frac{m_Z^2}{2} \left\{ 1 + \left[\cos^2 2\beta + \left(2\frac{m_W^2}{m_Z^2} - 1 \right) \sin^2 2\beta \right]^{1/2} \right\} \ . \tag{3.34}$$

The upper bound for $m_{S_2}^2$ [for which there is no $O(x)$ correction] results from the upper bound on λ given in Eq. (3.32). There is also an upper bound on λ coming from the requirement $m_{S_1}^2 \ge 0$:

$$\lambda^2 v^2 \le m_Z^2 + \frac{2 A_\lambda x m_Z}{v \sin 2\beta} \ . \tag{3.35}$$

However, this is clearly weaker than that of Eq. (3.32). Finally, we note that the requirement that the asymmetric vacuum be the global minimum (in particular, that it be a lower minimum than the symmetric vacuum) leads to a lower bound for λ. From Eq. (3.10), keeping terms up to $O(x)$, we find

$$\lambda^2 v^2 \ge 2 m_Z^2 \cot^2 2\beta + \frac{2\sqrt{2} A_\lambda x m_Z |\cos 2\beta|}{v \sin^2 2\beta} \ . \tag{3.36}$$

The two conditions on λ given in Eqs. (3.32) and (3.36) are in danger of being incompatible. This leads to restrictions on the other parameters of the model. Thus, at small x, Eqs. (3.32) and (3.36) are consistent only if

$$\cot^2 2\beta \le \frac{1}{2} \frac{m_W^2}{m_Z^2} + O(x^2) \ . \tag{3.37}$$

For example, in the $\tan\beta > 1$ sector this is equivalent to $\tan\beta \le 2.09$ up to corrections proportional to x.

IV. MASS-SPECTRA WITHOUT GUT-SCALE BOUNDARY CONDITIONS

In this section we shall give a sampling of the Higgs-boson mass spectra, subject to only the most basic requirements on the theory. The first requirement is that the vacuum expectation value of the potential, $\langle V_{\mathrm{neutral}} \rangle$, be negative at the symmetry-breaking extremum. This implies that the symmetry-breaking configuration defined by Eq. (2.16) is at least preferred over the local extremum where the vacuum expectation values of all Higgs fields are zero.[17] The second requirement is that this symmetry-breaking extremum be a local minimum of the Higgs potential, Eq. (2.10). This is guaranteed if all Higgs bosons have positive squared masses. Finally, one should require that there be no color- and charge-breaking minimum that is preferred over the color- and charge-conserving minima we examine. We shall first survey the possible local minima without this requirement. We shall then discuss the constraints coming from including it in a simplified form, neglecting intergenerational mixing and considering only the potential terms involving the third-generation squark doublet $\tilde{Q}$ and singlet $\tilde{U}^c$ (with the other squark singlet $\tilde{D}^c$ set to zero). Even with these simplifications, color-breaking restrictions will depend on the parameters h, A_h, $m_{\tilde{Q}}$, and $m_{\tilde{U}^c}$ associated with the colored degrees of freedom of the scalar poten-

tial. Here, h is the top-quark Yukawa coupling, A_h is the corresponding soft supersymmetry-breaking parameter, and $m_{\tilde{Q}}^2$ and $m_{\tilde{U}^c}^2$ give the soft supersymmetry-breaking mass terms for the fields $\tilde{Q}$ and $\tilde{U}^c$, respectively. For further details, see Appendix A. Additional restrictions might or might not be present depending upon the precise values of these parameters.

Turning now to the noncolored degrees of freedom, the parameters at our disposal are λ, k, r, $\tan\beta$, A_λ, and A_k. It is not possible to present a full exploration of the entire parameter space, and we impose the following restrictions on their values.

(1) We will focus on values of λ and k that are favored by the renormalization-group equations to be discussed in the following section. There are two classes of such values. First, it is easily demonstrated that there are fixed points for λ and k. If the GUT scale values for λ and k are of order 1 or larger, the low-energy values of these parameters will tend to be quite near their fixed-point values:

$$\lambda \simeq 0.87, \quad k \simeq 0.63 . \tag{4.1}$$

The second class of values is that obtained by imposing special boundary conditions at the unification scale. These tend to be characterized by substantially smaller values of λ and will be considered in more detail in the next section. The corresponding mass spectra will turn out to be much more restrictive than those obtained for the values of Eq. (4.1), and will be discussed in Sec. V.

(2) Next we discuss values of r [defined in Eq. (2.21)]. Since $x \neq 0$ does not break any gauge symmetry, the parameter $r = x/v$ is not constrained by neutral-current experiments. We shall consider three choices for our survey,

$$r = 0.1, 1.0, 10 , \tag{4.2}$$

although the latter choice will turn out to be quite disfavored in the renormalization-group analysis.

(3) The value of $\tan\beta$ is largely determined by the top-quark mass. We shall see in the following section that the renormalization-group analysis of radiative symmetry-breaking always leads to $\tan\beta$ values that are larger than 1. This result is not peculiar to the particular model that we are discussing; it appears to be a general feature of all phenomenologically viable theories that incorporate low-energy supersymmetry and radiative breaking of the electroweak symmetry.[18] For the purpose of illustrating the mass spectra, we shall take $\tan\beta = 1.5$ at each r value. To give a feeling of the sensitivity to $\tan\beta$, we shall also consider $\tan\beta = 4$ at $r = 1$. We also note that at $r = 0.1$ there are no allowed solutions once $\tan\beta \gtrsim 3.3$.

(4) Turning to the remaining parameters, we first note that, at fixed λ, k, r, and $\tan\beta$, a choice for A_λ determines the mass of the charged Higgs boson m_C. The remaining parameter A_k does not enter into m_C but must be specified in order to fix the masses of the Higgs scalar and pseudoscalar. Our procedure will be to explore the allowed range of m_C for the λ, k, r, and $\tan\beta$ values

specified earlier, (using m_C to fix the value of A_λ) and scan over all allowed values of A_k. As mentioned in Sec. II, the Higgs pseudoscalars are guaranteed to have positive mass squared, and the allowed range of A_k (recall $A_k > 0$ in our phase convention) will be determined by imposing

$$\langle V_{\text{neutral}} \rangle < 0, \quad m_{S_1}^2 > 0 . \tag{4.3}$$

Typically, there is a restricted range of m_C over which solutions are possible. Within this range $A_k = 0$ is always an allowed value and the maximum value of A_k is determined by failure to satisfy one of the constraints of Eq. (4.3). As A_k increases from 0, if $\langle V_{\text{neutral}} \rangle > 0$ is encountered before $m_{S_1}^2 < 0$, then there is a lower bound on m_{S_1}, whereas in the converse case the lower bound on m_{S_1} is 0.

Our results are presented in Figs. 1(a)–1(d). A number of features of these results are worthy of comment. First, we note that the $\tan\beta = 1.5$ results plotted are not very different from those obtained at $\tan\beta = 1$. (The smaller value of $\tan\beta$ yields slightly lower minimum and maximum m_C values for $r = 1$ and 10.) The graphs indicate that at small $r = 0.1$ there is never a nonzero lower bound on m_{S_1}, whereas at $r = 1$ and 10, there are regions of m_C where m_{S_1} cannot be zero. At $\tan\beta = 1.5$, $m_C = 0$ is allowed for $r = 0.1$, but for $r = 1$ or 10 there is a significant lower bound on m_C. At $r = 1$ the lower *and* upper bounds on m_C increase significantly in going from $\tan\beta = 1.5$ to $\tan\beta = 4$. In the following section we shall find that extreme values of r are disfavored for the simplest grand unification boundary conditions at m_{Pl}. Thus, the $r \lesssim 1$ results might be regarded as most interesting. For such r values, all Higgs-boson masses lie below 1 TeV for reasonable values of $\tan\beta$.

Nonetheless, it is interesting to see how closely the $r = 0.1$ and $r = 10$ numerical results correspond to the $r \to 0$ and $r \to \infty$ cases, respectively, studied in the previous section. We will only mention a few interesting points. Consider the $r \to 0$ limit. First, we observe in Fig. 1(a) that m_{P_2} and m_{S_3} are, indeed, approximately degenerate, as anticipated from the $r \to 0$ limit discussion. We also see from Fig. 1(a) that, for moderate $\tan\beta$, $m_C = 0$ is allowed but that m_C cannot exceed $\sim m_W$. This again agrees with our limiting case analysis. Also Fig. 1(a) reveals that m_{S_1} is always $< m_Z$, that m_{S_2} is of order m_Z, and that m_{S_3} is quite large, in agreement with Eqs. (3.33), (3.34), and (3.23), respectively. However, in one respect we are rather far from the strict $r \to 0$ limit. The fixed-point value of λ^2 that we are considering is quite a bit larger than the $r \to 0$ upper bound of $\frac{1}{2}g^2$ implied by Eq. (3.32), with $x = 0$. The reason for this is that the term proportional to $A_\lambda x$ is not small, since A_λ is large. Thus, our $r = 0.1$ results are not in a domain where the strict perturbative approach of Sec. III is applicable. For example, for the plots of Fig. 1(a) we typically find $A_\lambda \sim 500$ GeV, implying that the $A_\lambda x$ term of Eq. (3.32) is as large as the "leading" m_W^2 term. Indeed, if no upper bound on A_λ is imposed, there is no upper bound on λ in the $r \to 0$ limit.

Turning to the large-r limit, we note that by combining Eqs. (2.18) and a bound on m_C of the type found for $\tan\beta=1$ in Eq. (3.9), we predict that the charged-Higgs-boson mass should lie within a rather definite range of values. For instance, at $\tan\beta=1$ Eq. (3.9) predicts an upper bound on m_C of ~ 3600 GeV, for the fixed-point values of λ and k and for $r=10$. We see from Fig. 1(c) that this is rather close to the $\tan\beta=1.5$ numerical result. Similarly, the rough limit of $A_k \leq 3kx$ obtained from Eq. (3.10) is found to be approximately correct in our numerical scan at $r=10$. Finally, we observe from our figures that there are indeed two rather massive scalar Higgs-boson states, and that only S_1 can be relatively light at large r, in agreement with Eqs. (3.1)–(3.3).

Let us now return to the question of whether or not there are minima of the scalar potential that break charge and/or color and that are lower than the local minima we have examined above. Consider first the question of charge breaking in the sector of the scalar potential not involving colored fields. Any one of the local minima as-

sociated with the curves plotted above has completely determined values for all the parameters appearing in the scalar potential of Eq. (2.2). We may then search for charge-breaking minima that have a lower value of V_{Higgs}. This occurs if the vacuum expectation values appearing in Eq. (2.13) can readjust themselves in such a way that V_{Higgs} is more negative while at the same time the (negative) $m_{H_2}^2$ term overtakes the other terms, and the coefficient of $|v^-|^2$ in Eq. (2.12) becomes negative. Indeed, we find that this does occur for some of the local minima solutions plotted earlier. The effect on the mass spectra is not, however, very marked. The primary result is the elimination of the lowest charged-Higgs-boson mass solutions for a given value of r. For instance, for the fixed point λ and k values, at $r=0.1$, m_C values below ~ 5 GeV are eliminated, while at $r=1$, m_C values below ~ 170 GeV yield a preferred charge-breaking minimum. We expect the solutions with m_C near 0 in the $r=0.1$ case to be modified by Coleman-Weinberg[19] loop corrections in any case. In addition, we find that the
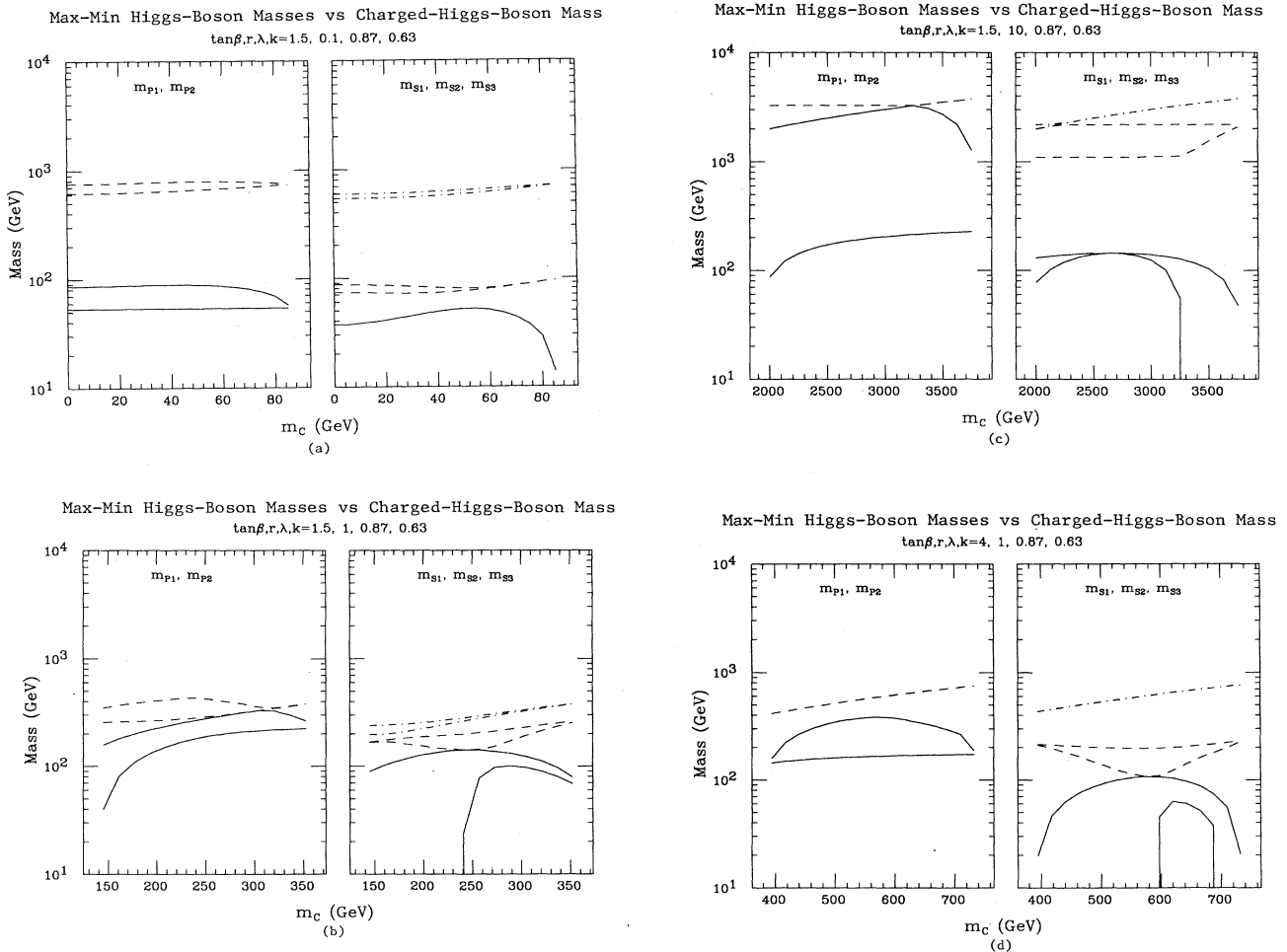

FIG. 1. Maximum and minimum masses for the neutral Higgs bosons as a function of the charged-Higgs-boson mass m_C. For m_C values outside the range plotted there are no allowed solutions satisfying Eq. (4.3). We have taken $\lambda=0.87$, $k=0.63$, and (a) $r=0.1$, $\tan\beta=1.5$; (b) $r=1$, $\tan\beta=1.5$; (c) $r=10$, $\tan\beta=1.5$; (d) $r=1$, $\tan\beta=4$.

charge-breaking minimum is generally only 10–20% below the charge-conserving local minimum, so that tunneling would be slow. Therefore, in our coupling constant plots to be given later, we will retain all solutions with charge-conserving local minima.

We now consider including the colored degrees of freedom, as discussed in more detail in Appendix A. We will assume that the colored fields are all parallel in color space. Any conditions that we obtain in order to avoid color breaking will therefore by only necessary and not sufficient. However, we note that the SU(3) D term (see Appendix A) tends to prefer the parallel configuration. Of course, a full renormalization-group analysis within the context of the model and with definite grand unification boundary conditions is required in order to determine the various parameters associated with the colored degrees of freedom of the scalar potential relative to those we have already considered. Examples of such scenarios will be considered in the following section. Here, we confine ourselves to picking a particular local minimum among those found earlier, and computing the boundary in $A_h^2 - m_{\tilde{Q}}^2$ space (for fixed h) which separates the region where color breaking is preferred from the region where the particular local minimum being considered is the true global minimum. We have chosen to examine the local minimum specified by the following parameters: $r = 1$, $\tan\beta = 1.5$, $\lambda = 0.83$, $k = 0.67$, $m_C = 220$ GeV (corresponding to $A_\lambda = 88.4$ GeV), $A_k = 303$ GeV. In addition, we shall choose $h = 0.5$; this is in the general range given by the renormalization-group solutions considered later. We have also chosen to take $m_{\tilde{U}^c}^2 = m_{\tilde{Q}}^2$. The boundary is given in Fig. 2. Typically, when color breaking is preferred, the colored field vacuum expectation values u and u^c (of the left- and right-handed stop fields) are nonzero and roughly equal. The only other

large vacuum expectation value for these minima is v_2, which increases as one moves along the upper (color breaking) side of the boundary in the direction of larger A_h. Not surprisingly, it is these three vacuum expectation values that occur in association with the hA_h term in V_{soft}, as given in Appendix A. Various suggestions have appeared in the literature[20] as to what types of conditions guarantee that color breaking is not preferred. Our results do not appear to correspond to any of these previous suggestions. They appear to follow more along the lines of the considerations given in Ref. 21; as shown there, additional subtleties associated with negative mass-squared terms in the soft supersymmetry-breaking potential, and spontaneous symmetry breaking, invalidate the naive bounds.

V. RENORMALIZATION-GROUP ANALYSIS

In this section we consider the constraints imposed by the renormalization-group equations (RGE's) on the parameters of the scalar potential. First, we point out the existence of infrared fixed points for the superpotential parameters λ and k, which can be taken as upper bounds on their possible experimental values. Then we make a more detailed analysis of the parameter values which lead to an acceptable pattern of electroweak symmetry breaking and sparticle masses, assuming that supersymmetry breaking can be parametrized at the grand unification scale by a universal gaugino mass term, with the other soft supersymmetry-breaking terms generated by radiative corrections. These preferred parameter values are then used in the general formulas of Sec. II to make specific predictions for the Higgs-boson masses within the ranges allowed by the general analysis of Sec. IV. Very stringent constraints on the sparticle masses and on the top-quark mass are also obtained.

The renormalization-group equations for our model can be trivially obtained from Ref. 13 and will not be reported here. Let us only stress again our earlier remark about linear and bilinear terms in the soft supersymmetry-breaking potential: examining the structure of the renormalization-group equations for such terms one can check that, if they are absent at one scale, then they must be zero at every scale, provided there are no linear or bilinear superpotential terms. In employing the renormalization-group equations, we make the usual approximation of neglecting intergenerational mixing and the Yukawa couplings of the light quarks and leptons, keeping only λ, k, the top Yukawa coupling h and their soft potential counterparts. It is consistent to neglect the bottom-quark Yukawa coupling as long as $\tan\beta \ll m_t/m_b$. The parameters that we evolve are therefore the gauge couplings g_A and the gaugino masses M_A [$A = 3,2,1$ corresponds to SU(3)$_C$, SU(2)$_L$, and U(1)$_Y$, respectively], the Yukawa couplings h, λ, k and the corresponding trilinear scalar couplings and soft scalar masses, A_h, A_λ, A_k and $m_{\tilde{Q}}^2, m_{\tilde{U}^c}^2, m_{H_1}^2, m_{H_2}^2, m_N^2$. It is customary to assume the following boundary conditions at the unification scale M_X:

Color-Breaking Boundary
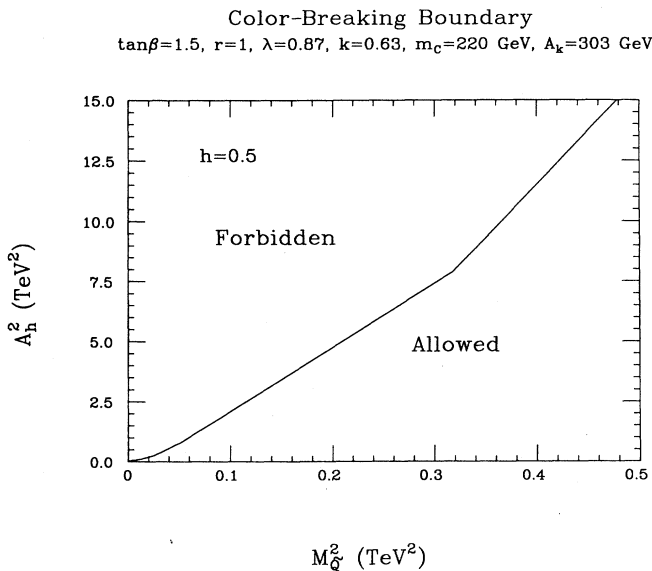$\tan\beta = 1.5$, $r = 1$, $\lambda = 0.87$, $k = 0.63$, $m_C = 220$ GeV, $A_k = 303$ GeV

FIG. 2. Color-breaking boundary in $A_h^2 - m_{\tilde{Q}}^2$ space. For details see text.

$$g_1 = g_2 = g_3 \equiv g_U \ ,$$

$$M_1 = M_2 = M_3 \equiv M_U \ ,$$

$$h = h_U, \quad \lambda = \lambda_U, \quad k = k_U \ , \qquad (5.1)$$

$$m_Q^2 = m_{U^c}^2 = m_{H_1}^2 = m_{H_2}^2 = m_N^2 \equiv m_U^2 \ ,$$

$$A_h = A_\lambda = A_k \equiv A_U \ .$$

In our renormalization-group equations, we distinguish between two different regimes. We call M_{SUSY} the typical scale of the dominant soft supersymmetry-breaking terms. For reasons to be discussed below, we will assume that $M_U \gg m_U, A_U$. Hence, we can identity M_{SUSY} with the gluino mass $m_{\tilde{g}} \equiv M_3$, and we must have $M_{\mathrm{SUSY}} \simeq m_{\tilde{g}} \gtrsim 140$ GeV to avoid unacceptably small slepton masses. For renormalization scales Q between M_{SUSY} and M_X we use the supersymmetric one-loop renormalization-group equations, which are known to be a good approximation when $M_{\mathrm{SUSY}} \ll Q$. A precise treatment of all the different particle thresholds around and below M_{SUSY} would be very complicated. To simplify life, we compute all the soft supersymmetry-breaking parameters and minimize the effective potential at $Q = M_{\mathrm{SUSY}}$. To establish the connection with the low-energy values of the gauge couplings and of the top-quark mass, we use nonsupersymmetric renormalization-group equations between m_W and M_{SUSY} (Ref. 22).

We note that, in the supersymmetric one-loop approximation, the evolution of the dimensionless couplings is not affected by the soft supersymmetry-breaking parameters. This allows us to identify nontrivial infrared fixed points for the Yukawa couplings λ and k, corresponding to the initial values $\lambda_U, k_U \rightarrow \infty$. For $Q = M_{\mathrm{SUSY}} \simeq m_W$, we find

$$\lambda \simeq 0.87, \quad k \simeq 0.63 \ . \qquad (5.2)$$

These values can be taken as upper limits on λ and k, as was already done in Sec. IV.

In the following, we will restrict ourselves to a particularly simple choice of boundary conditions:

$$M_U \neq 0, \quad m_U, A_U = 0 \ , \qquad (5.3)$$

so that supersymmetry breaking can be described in terms of the single parameter M_U. While (5.3) seems to be favored in some superstring-inspired supergravity models,[23] the main motivation for assuming (5.3) here is its simplicity.[24] We note that we must choose M_U to be positive in order to generate positive A_λ and A_k values (as required in our conventions) beginning with the boundary condition $A_U = 0$. If we recall from the introduction, Eq. (1.7), that the effective μ parameter corresponding to that of the minimal supersymmetric model is positive in the conventions of this paper, we see that the renormalization-group equations with boundary conditions (5.3) imply that the gaugino mass and the effective μ parameter must have the same sign. This is to be contrasted with the minimal supersymmetric model[3] where, in general, one must also allow for μ to have sign opposite to that of the gaugino mass.

We now describe in detail our renormalization-group analysis. Using as physical input the values $\alpha_{\mathrm{em}}(m_W)$ and $\alpha_3(m_W)$, we compute the unification mass M_X, the unification coupling $\alpha_U \equiv g_U^2/4\pi$ and $\sin^2\theta_W(m_W)$ as a function of M_{SUSY}. For instance, for $\alpha_{\mathrm{em}}(m_W) = 1/127.9$, $\alpha_3(m_W) = 0.115$, and $M_{\mathrm{SUSY}} = 200$ GeV we find

$$M_X = 1.4 \times 10^{16} \text{ GeV}, \quad \alpha_U = \frac{1}{24.9} \ ,$$
$$\sin^2\theta_W(m_W) = 0.231 \ . \qquad (5.4)$$

Then, for any given set of boundary values (h_U, λ_U, k_U), we compute all the relevant parameters at the scale $Q = M_{\mathrm{SUSY}}$. After checking that our phase conventions $\lambda A_\lambda > 0, k A_k > 0$ are satisfied, and that $\lambda, k > 0$ in order to avoid spontaneous CP breaking, we perform a computer search for a global minimum of the neutral Higgs potential (2.11). Then, we include charge and colored degrees of freedom in the scalar potential (as described in Appendix A) and check that the complete effective potential does not have minima of lower energy which break color and/or electric charge. Moreover, we keep only minima which satisfy the following conditions:

$$x, v_1, v_2 \neq 0 \ , \qquad (5.5)$$

$$\frac{1}{20} < \frac{x}{(v_1^2 + v_2^2)^{1/2}}, \frac{v_1}{(x^2 + v_2^2)^{1/2}}, \frac{v_2}{(v_1^2 + x^2)^{1/2}} < 20 \ .$$

This allows us to give masses to all quarks, leptons, and Higgs bosons and prevents instabilities with respect to radiative corrections and/or small variations of the renormalization scale $Q \simeq M_{\mathrm{SUSY}}$. Up to this point, the procedure is independent of the primordial gaugino mass M_U, which can be factorized out of the renormalization-group equations and of the effective potential. We then fix M_U by requiring

$$m_W^2 = \frac{g_2^2(m_W)}{2}(v_1^2 + v_2^2) = 81 \text{ GeV} \ . \qquad (5.6)$$

Then we compute the complete spectrum of the model, and we verify that the following phenomenological constraints are satisfied.

Constraints on slepton masses. We require

$m_{\tilde{\nu}}^2 > 0$ to avoid a $\Delta L \neq 0$ vacuum ,

$m_{\tilde{e}_L}, m_{\tilde{e}_R} > 25$ GeV as required by e^+e^- data

$$(\text{Ref. 25}) \ , \qquad (5.7)$$

$(m_{\tilde{e}_L}^2 + m_{\tilde{\nu}}^2)^{1/2} > 47$ GeV as required by UA1 data

$$(\text{Ref. 26}) \ .$$

Constraint on chargino masses. Denoting by $\tilde{\chi}_1^+$ the lightest chargino eigenstate, we require

$m_{\tilde{\chi}_1^+} > 25$ GeV as required by e^+e^- data

$$(\text{Ref. 25}) \ . \qquad (5.8)$$

ASP constraint. This experiment puts a combined limit on the masses of the charged sleptons and of the lightest neutralino, denoted here by $\tilde{\chi}_1^0$. A sufficient condition to avoid any conflict with the ASP data is[27]

$$[m_{\tilde{e}_{L,R}}^2 + (6m_{\tilde{\chi}_1^0})^2]^{1/2} > 65 \text{ GeV} . \tag{5.9}$$

Constraints on squark and gluino masses. To avoid any conflict with the limits imposed by UA1 and UA2 data,[28] we require

$$m_{\tilde{g}} > 70 \text{ GeV}, \quad m_{\tilde{q}} > 70 \text{ GeV} . \tag{5.10}$$

Moreover, in order to avoid instabilities in the effective potential we impose[29]

$$m_{\tilde{g}}, m_{\tilde{q}} < 500 \text{ GeV} . \tag{5.11}$$

Two important consistency tests on the spectra are the following. After computing the top-quark mass, we verify that the condition $\tan\beta \ll m_t/m_b$ is satisfied and that $45 \text{ GeV} < m_t < 200 \text{ GeV}$, as required by UA1 (Ref. 30) and neutral-current data.[31] After computing the gluino mass $m_{\tilde{g}}$ (from M_U through the renormalization-group equations) we verify that $M_{\text{SUSY}} \sim m_{\tilde{g}}$. Both tests are satisfied by all our solutions. Since the typical gluino masses are between 140 and 260 GeV, our results are given for $M_{\text{SUSY}} = 200 \text{ GeV}$.

After observing that the properties of the electroweak vacuum are mainly determined by h_U and λ_U, while a wide range of k_U values is allowed, we have used for our searches an array of (h_U, λ_U) values, for the three representative values: (a) $k_U = 0.01$; (b) $k_U = 0.1$; and (c) $k_U = 1$. The region of the (h_U, λ_U) plane which gives vacua satisfying all the constraints is given by the area in Figs. 3(a)–3(c) labeled by the large capital A. The solid line delimits the regions where charge- and color-conserving vacua satisfying Eq. (5.5) can be obtained. For values of h_U that are too small and/or for values of λ_U that are too large, one is unable to satisfy Eq. (5.5), while values of h_U greater than ~ 0.18 tend to generate charge-breaking minima: as we will see, this puts strong constraints on the top-quark mass. The regions denoted by the letter B are excluded by the constraints (5.7) on the slepton masses, and the regions denoted by the letter C are excluded by the constraint (5.8) on the lightest chargino mass. The constraints (5.9), (5.10), and (5.11) are weaker and do not restrict further the allowed region. Typical ranges of variation for the most relevant parameters, corresponding to allowed solutions, are collected in Table I.

A number of comments are in order. As apparent from the restricted range of acceptable h_U (or h) values, the allowed range of m_t is strongly constrained

$$75 \text{ GeV} \leq m_t \leq 93 \text{ GeV} . \tag{5.12}$$

Of course, one has to keep in mind that this prediction is a consequence of the boundary conditions (5.3) and could be slightly weakened when taking into account threshold effects, higher-loop corrections and uncertainties in the input parameters $\alpha_{\text{em}}(m_W)$ and $\alpha_3(m_W)$. Also, the al-
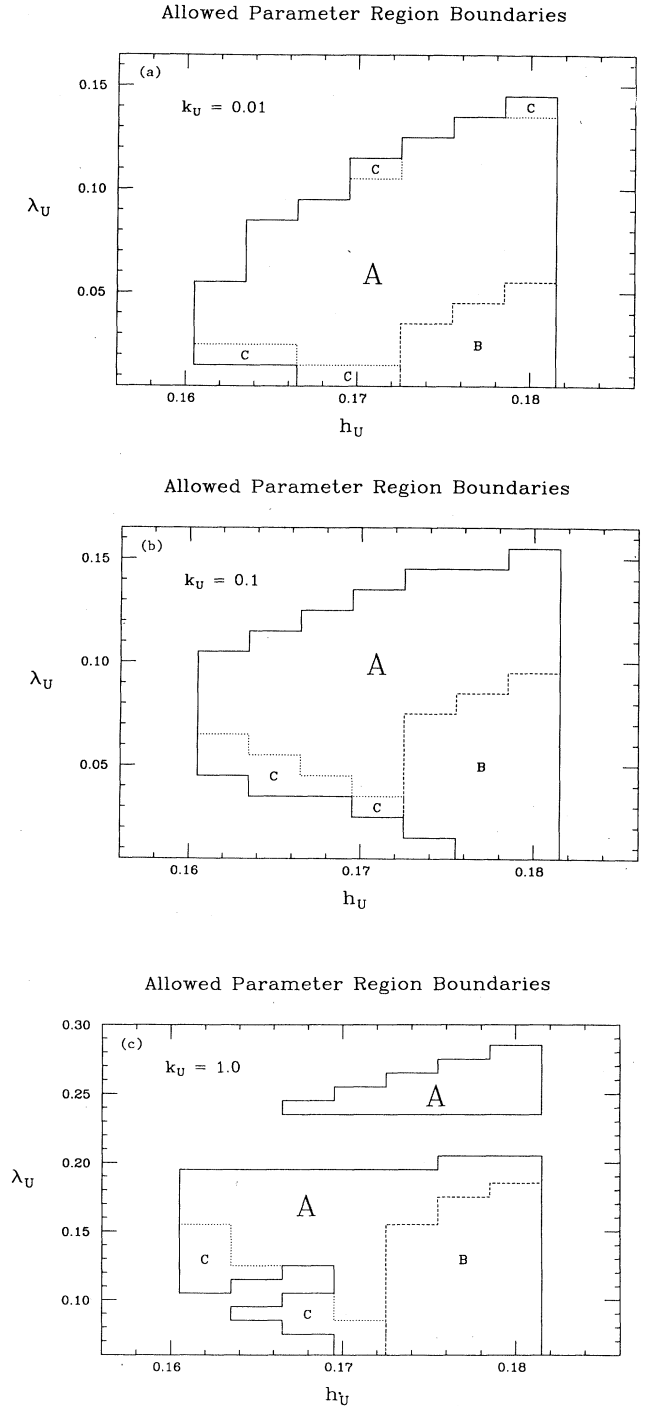
Allowed Parameter Region Boundaries

Allowed Parameter Region Boundaries

Allowed Parameter Region Boundaries

FIG. 3. Region of the (h_U, λ_U) plane allowed by the different constraints discussed in the text. The region within the solid outline corresponds to h_U, λ_U values that give charge- and color-conserving vacua, which also satisfy Eq. (5.5). Within this region the constraint on the slepton masses, Eq. (5.7), removes regions labeled by the letter B (outlined by dashes) and the constraint on the lightest chargino mass, Eq. (5.8), removes the regions labeled by the letter C (outlined by dots). The remaining fully acceptable solution region is indicated by the large capital A. Three representative values of k_U have been considered: (a) $k_U = 0.01$; (b) $k_U = 0.1$; and (c) $k_U = 1$.

lowed minima correspond to relatively light sparticle masses

$$m_{\tilde{g}} \leq 260 \text{ GeV}, \quad m_{\tilde{q}} \leq 240 \text{ GeV} ,$$

$$m_{\chi_1^+} \leq 64 \text{ GeV}, \quad m_{\chi_1^0} \leq 36 \text{ GeV} , \qquad (5.13)$$

$$m_{\tilde{v}} \leq 37 \text{ GeV}, \quad m_{\tilde{e}_L} \leq 85 \text{ GeV}, \quad m_{\tilde{e}_R} \leq 57 \text{ GeV} .$$

These results should give encouragement to physicists at the Fermilab Tevatron collider, CERN LEP, and SLAC Linear Collider (SLC). To reemphasize, the demand that the renormalization-group evolution yield an acceptable scalar particle sector (with the observed electroweak symmetry breaking, and no charge or color breaking) has led to a highly constrained spectrum for all the remaining particles of the model.

Passing now to the Higgs sector, on which the present analysis is focused, we see that many Higgs bosons are light enough to contemplate searches for them at LEP and SLC. Note, however, that all our solutions correspond to squark and gluino masses safely above the range of values which should soon be excluded by the CDF ex-

periment at the Tevatron. Furthermore, the lightest mass generated by the renormalization-group equations for the scalar S_1 is 4.6 GeV (Ref. 32), so that it escapes the CUSB limits.[33] Moreover, S_1 can contain a significant N component, so that its couplings and possible radiative corrections to its mass can be considerably weaker than in the minimal case. Also S_2 and the lightest pseudoscalar P_1 can be significantly lighter than the Z. The charged Higgs boson is never lighter than the W, but never heavier than the Z: this depends on the fact that relatively small values of λ ($\lambda \leq 0.28$) are favored by our solutions. The phenomenological prospects in experimental searches for these Higgs bosons will be discussed in detail in the following sections. Two more comments on our results are in order. First, our solutions never allow r to be substantially larger than 1 and, indeed, $r < 1$ is favored (see Table I): this is related to the fact that $x \gg v_1, v_2$ requires m_N^2 to be negative and large, which can never occur if the singlet N can have only the small Yukawa couplings λ and k. Second, the lightest supersymmetric particle (LSP) can be either the sneutrino $\tilde{v}$ or the neutralino $\tilde{\chi}_1^0$: the first possibility is favored for high values of λ, the second for small values of λ. The lightest neutralino $\tilde{\chi}_1^0$ is in general a full mixture of $\tilde{H}_1$, $\tilde{H}_2$, $\tilde{N}$, $\tilde{W}_3$, and $\tilde{B}$, with a dominant $\tilde{H}_2$ component.

A few final observations are appropriate before closing this section. We have seen that the assumption of the boundary conditions (5.3) implies $\lambda \leq 0.28$ (substantially lower than the fixed-point value), $r \leq 1.7$, and $k \leq 0.54$. It is interesting to ask to what extent the renormalization-group restrictions on the remaining parameters are stronger than those imposed by the general constraints of Eq. (4.3). In order to explore this question we have focused on a representative solution of the renormalization-group equations. For the initial values $h_U = 0.171$, $\lambda_U = 0.1$, $k_U = 0.1$, we obtain, at $M_{\text{SUSY}} = 200$ GeV,

$$\lambda = 0.128, \quad k = 0.097, \quad r = 0.64, \quad \tan\beta = 2.04 , \qquad (5.14)$$

and

TABLE I. Typical ranges of parameters and masses for the allowed solution regions of Fig. 3, obtained assuming that gaugino masses are the dominant source of supersymmetry breaking at the unification scale.

Parameter	$k_U = 0.01$	$k_U = 0.1$	$k_U = 1.0$
h_U	0.16–0.18	0.16–0.18	0.16–0.18
λ_U	0.01–0.14	0.03–0.16	0.08–0.29
h	0.48–0.52	0.48–0.52	0.48–0.53
λ	0.058–0.15	0.077–0.18	0.11–0.28
k	0.01	0.096–0.10	0.51–0.54
A_h (GeV)	160–310	160–310	160–310
A_λ (GeV)	19–38	18–38	18–37
A_k (GeV)	0.03–1.3	0.13–1.5	0.94–2.9
m_t (GeV)	76–93	76–91	75–89
$\tan\beta$	1.4–4.4	1.4–4.2	1.4–4.2
r	0.28–1.7	0.34–0.67	0.25–0.40
$m_{\tilde{g}}$ (GeV)	140–260	140–260	140–260
$m_{\tilde{q}}$ (GeV)	110–240	110–240	110–240
$m_{\tilde{v}}$ (GeV)	6.1–37	4.0–36	1.8–36
$m_{\tilde{e}_L}$ (GeV)	46–85	47–85	47–85
$m_{\tilde{e}_R}$ (GeV)	32–57	33–57	33–57
$m_{\chi_1^+}$ (GeV)	25–63	25–63	25–64
$m_{\chi_1^0}$ (GeV)	4.8–27	5.9–32	10–36
m_C (GeV)	81–89	82–90	83–90
m_{P_1} (GeV)	4.7–9.3	21–33	28–52
m_{P_2} (GeV)	23–44	27–49	49–94
m_{S_1} (GeV)	4.6–17	5.5–20	5.8–25
m_{S_2} (GeV)	12–40	30–48	60–85
m_{S_3} (GeV)	93–95	93–95	93–98

Max-Min Higgs-Boson Masses vs Charged-Higgs-Boson Mass
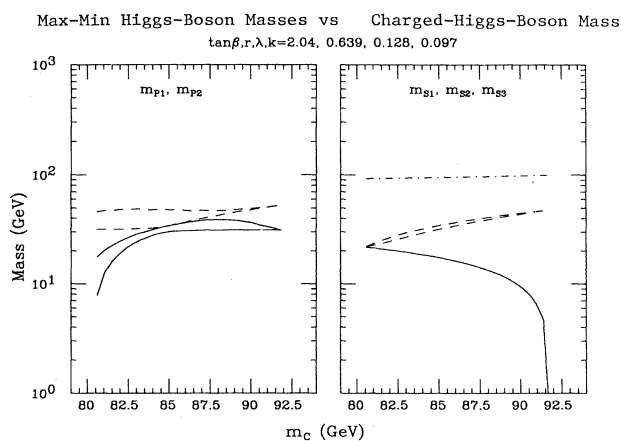tanβ,r,λ,k=2.04, 0.639, 0.128, 0.097

FIG. 4. Higgs-boson mass spectra as a function of m_C, for the parameter choices of Eq. (5.14): $\lambda = 0.128$, $k = 0.097$, $r = 0.64$, $\tan\beta = 2.04$.

TABLE II. The Higgs-boson and sparticle masses for a representative solution of our renormalization-group equation constraints: $\lambda=0.128$, $k=0.097$, $r=0.64$, $\tan\beta=2.04$, $A_\lambda=28.6$ GeV, $A_k=0.7$ GeV (corresponding to $h_U=0.171$, $\lambda_U=0.1$, $k_U=0.1$, and $M_{\rm SUSY}=200$ GeV).

Particle	Mass (GeV)	Particle	Mass (GeV)
S_1	15	$m_{\tilde{\nu}}$	23
S_2	38	$m_{\tilde{e}_L}$	67
S_3	95	$m_{\tilde{e}_R}$	46
P_1	31	$m_{\tilde{\chi}_1^+}$	49
P_2	39	$m_{\tilde{\chi}_2^+}$	123
$C^\pm$	86	$m_{\tilde{\chi}_1^0}$	23
m_t	83	$m_{\tilde{\chi}_2^0}$	33
$m_{\tilde{g}}$	204	$m_{\tilde{\chi}_3^0}$	36
$m_{\tilde{q}}$	177	$m_{\tilde{\chi}_4^0}$	78
$m_{\tilde{t}_1}$	130	$m_{\tilde{\chi}_5^0}$	120
$m_{\tilde{t}_2}$	229		

$$A_\lambda=28.6 \text{ GeV}, \quad A_k=0.7 \text{ GeV} . \tag{5.15}$$

The Higgs boson and sparticle masses obtained for this solution are given in Table II. To investigate how restrictive for the Higgs-boson masses the λ,k,r values of Eq. (5.14) are, we now ignore the specific results of Eq. (5.15) from the renormalization-group equations and scan in m_C and A_k in the manner of the earlier analyses of the fixed point λ,k values. In Fig. 4 we display the mass spectra of the pseudoscalar and scalar Higgs bosons for the values of $\lambda,k,r,\tan\beta$ of Eq. (5.14), but with no restriction on A_λ and A_k. From this figure, it is clear that the small values of λ and r generated by the renormalization-group equations in the above special case allow only for a very narrow range of possible Higgs-boson masses in contrast with the large λ values explored in Sec. IV.

VI. HIGGS-BOSON COUPLINGS

In this section we discuss the various couplings of the Higgs bosons that are of primary phenomenological interest. In particular, we shall be interested in the extent to which the phenomenology of the present model deviates from that of minimal supersymmetry and E_6 string based models. The latter models have been explored in detail in Refs. 3, 15, and 34.

We will explore four basic classes of Higgs-boson coupling: (a) couplings of a Higgs boson to vector-boson pairs; (b) couplings of a Higgs boson to quark pairs; (c) couplings of a Higgs boson to another Higgs boson and a vector boson; and (d) self-couplings of the Higgs bosons. We shall employ the formulation discussed in Ref. 34, which makes use of the Higgs eigenvector notation $H(j)$ ($j=1,2,3$ for H_1^0, H_2^0, and N components, respectively).

In order to obtain Feynman rules, the couplings quoted below should be multiplied by i; the appropriate combinatoric factors are already included.

A. HVV couplings

When CP is conserved, the Higgs pseudoscalars have no VV couplings. The VV couplings of the scalar Higgs bosons are

$$g_{S_a W^+ W^-} = gm_W(\cos\beta\mathcal{S}_a^1+\sin\beta\mathcal{S}_a^2)g^{\mu\nu} ,$$

$$g_{S_a ZZ} = \frac{gm_Z}{\cos\theta_W}(\cos\beta\mathcal{S}_a^1+\sin\beta\mathcal{S}_a^2)g^{\mu\nu} , \tag{6.1}$$

where $a=1,2,3$ for S_1, S_2, or S_3, respectively, and μ and ν are the Lorentz indices for the two vector bosons. Note that the sum of the squared couplings is equal to the standard-model result, due to the orthonormality of the S_a states.

B. $Hq\bar{q}'$ couplings

All the Higgs bosons have couplings to quark-antiquark pairs. The couplings are summarized by the following formulas. First, for neutral Higgs bosons we have

$$g_{S_a u\bar{u}}=\frac{-gm_u}{2m_W}\frac{\mathcal{S}_a^2}{\sin\beta}, \quad g_{P_\alpha u\bar{u}}=\frac{i\gamma_5 gm_u}{2m_W}\frac{\mathcal{P}_\alpha^2}{\sin\beta} ,$$

$$g_{S_a d\bar{d}}=\frac{-gm_d}{2m_W}\frac{\mathcal{S}_a^1}{\cos\beta}, \quad g_{P_\alpha d\bar{d}}=\frac{i\gamma_5 gm_d}{2m_W}\frac{\mathcal{P}_\alpha^1}{\cos\beta} , \tag{6.2}$$

where u and d are generic up- and down-type quarks, $a=1,2,3$, and $\alpha=1,2$, for the Higgs scalar and pseudoscalar, respectively. For the charged Higgs boson, we find

$$g_{C^- u\bar{d},C^+ d\bar{u}} = \frac{g}{2\sqrt{2}m_W}[(m_d\tan\beta+m_u\cot\beta)$$

$$\pm(m_d\tan\beta-m_u\cot\beta)\gamma_5] . \tag{6.3}$$

C. HHV couplings

Once again, we can use the eigenvector notation to succinctly summarize these couplings. We adopt the convention that all momenta and particles are incoming. We will use μ to denote the Lorentz index of the vector boson. For $W^-C^+(p')S_a(p)$ ($a=1,2,3$) we have

$$g_{W^\mp C^\pm S_a} = \frac{\pm g}{2}(p-p')^\mu(\mathcal{S}_a^2\cos\beta-\mathcal{S}_a^1\sin\beta) . \tag{6.4}$$

For $W^-C^+(p')P_\alpha(p)$ ($\alpha=1,2$) we have

$$g_{W^\mp C^\pm P_\alpha} = \frac{-ig}{2}(p-p')^\mu(\mathcal{P}_\alpha^2\cos\beta+\mathcal{P}_\alpha^1\sin\beta) . \tag{6.5}$$

For $ZS_a(p')P_\alpha(p)$ ($a=1,2,3$, $\alpha=1,2$) the coupling is

$$g_{ZS_a P_\alpha} = \frac{ig}{2\cos\theta_W}(p-p')^\mu(\mathcal{P}_\alpha^2\cos\beta+\mathcal{P}_\alpha^1\sin\beta)$$

$$\times(\mathcal{S}_a^2\cos\beta-\mathcal{S}_a^1\sin\beta) . \tag{6.6}$$

Finally, for $ZC^+(p')C^-(p)$ and $\gamma C^+(p')C^-(p)$ we obtain

$$g_{ZC^+C^-} = \frac{g\cos2\theta_W}{2\cos\theta_W}(p-p')^\mu \, ,$$

$$g_{\gamma C^+C^-} = e(p-p')^\mu \, .$$

$$(6.7)$$

D. HHH couplings

In summarizing the Higgs-boson self-couplings, it will be convenient to establish a notation closely related (but not identical) to that in Ref. 34. Using the pseudoscalar and scalar eigenvector matrices $\mathcal{P}_\alpha^j$ ($\alpha=1,2$) and $\mathcal{S}_a^j$ ($a=1,2,3$) where j can take on the values 1,2,3, and the charged Higgs eigenvectors $\mathcal{C}_+^l, \mathcal{C}_-^l$, $l=1,2$, of Eq. (2.33), we define the symbols

$$\Pi_{abc}^{ijk} \equiv \sum_{a,b,c \text{ perms}} \mathcal{S}_a^i \mathcal{S}_b^j \mathcal{S}_c^k \, ,$$

$$\Pi_{a\beta\gamma}^{ijk} \equiv \mathcal{S}_a^i (\mathcal{P}_\beta^j \mathcal{P}_\gamma^k + \mathcal{P}_\gamma^j \mathcal{P}_\beta^k) \, ,$$

$$\Pi_{a+-}^{ijk} \equiv \mathcal{S}_a^i (\mathcal{C}_+^j \mathcal{C}_-^k + \mathcal{C}_-^j \mathcal{C}_+^k) \, .$$

$$(6.8)$$

In Π_{abc}, a,b,c can take on values from 1 to 3. In $\Pi_{a\beta\gamma}$, a can take on values from 1 to 3, while β,γ range from 1 to 2. Finally, in Π_{a+-}, a can take on values from 1 to 3. It should be noted that in the above definitions, all sums are to be performed *regardless of whether or not some of the* a,b,c,β,γ, or i,j,k are equal. For example, in the case of all scalars $\Pi_{123}^{333} = 6\mathcal{S}_1^3\mathcal{S}_2^3\mathcal{S}_3^3$ and $\Pi_{111}^{333} = 6(\mathcal{S}_1^3)^3$. Because the expression for the Higgs-boson trilinear self-couplings are somewhat lengthy, we defer them to Appendix B. Contributions to the self-couplings arise from all the terms of the scalar potential of Eqs. (2.3)–(2.6).

E. Results for couplings in special limiting cases

In Sec. III we considered several limiting cases of our model. In this section we discuss results in these same limits for some of the Higgs couplings of interest. At large x, simple expressions for all couplings are possible, while at small x we shall focus only on those involving vector bosons, since the quark couplings do not take an especially simple form. In quoting results for the quark couplings we factor out the common expressions $-igm_q/(2m_W)$ or $-g\gamma_5/(2m_W)$ which appear in Eq. (6.2). For the vector-boson couplings, as given in Eqs. (6.1) and (6.4)–(6.6), we present the results by retaining only the factors in brackets in the above equations. We will denote the relative coupling strengths so obtained by the symbol $R\cdots$, where the subscript will indicate the particular coupling considered. For example, we define

$$g_{S_a W^+W^-} \equiv gm_W R_{S_a W^+W^-} \, ,$$

$$g_{W^-C^+S_a} \equiv \frac{g}{2}(p-p')^\mu R_{W^-C^+S_a} \, ,$$

$$g_{P_\alpha u\bar{u}} \equiv \frac{i\gamma_5 gm_u}{2m_W} R_{P_\alpha u\bar{u}} \, ,$$

$$g_{ZS_a P_\alpha} \equiv \frac{ig}{2\cos\theta_W}(p-p')^\mu R_{ZS_a P_\alpha} \, .$$

$$(6.9)$$

1. Limit of $x \gg v_1, v_2$ (λ, k fixed)

We use the explicit form of the Higgs-scalar mixing matrix given in Eq. (3.4) to compute the Higgs-scalar couplings. From the formulas given in the previous subsections, the couplings of interest are easily obtained. Consider first the couplings involving vector bosons. In the large-x limit we find

$$R_{W^-C^+S_i}, R_{ZP_2S_1} = O\left[\frac{1}{x^2}\right] \, ,$$

$$(6.10)$$

$$R_{W^-C^+P_2}, R_{W^-C^+S_2}, R_{ZP_2S_2} = 1 + O\left[\frac{1}{x^2}\right] \, ,$$

$$(6.11)$$

$$R_{W^-C^+S_3}, R_{ZP_2S_3} \sim \frac{\lambda v(k + A_\Sigma/x)\cos2\beta}{2kx\left[\dfrac{\lambda}{\sin2\beta} - 2k\right]} \, ,$$

$$(6.12)$$

and

$$R_{S_1 W^+W^-}, R_{S_1 ZZ} = 1 + O\left[\frac{1}{x^2}\right] \, ,$$

$$(6.13)$$

$$R_{S_2 W^+W^-}, R_{S_2 ZZ} = O\left[\frac{1}{x^2}\right] \, ,$$

$$(6.14)$$

$$R_{S_3 W^+W^-}, R_{S_3 ZZ} \sim \frac{\lambda}{4k^2x}v[2\lambda - (k + A_\Sigma/x)\sin2\beta] \, .$$

$$(6.15)$$

For the quark couplings we obtain

$$R_{S_1 u\bar{u}}, R_{S_1 d\bar{d}} \sim 1 \, ,$$

$$(6.16)$$

$$R_{S_2 u\bar{u}}, -R_{P_2 u\bar{u}} \sim \cot\beta \, ,$$

$$(6.17)$$

$$R_{S_2 d\bar{d}}, R_{P_2 d\bar{d}} \sim -\tan\beta \, .$$

$$(6.18)$$

We remind the reader that the pseudoscalar state P_1 not appearing in the above equations is that which decouples from nonsinglet fields, as does S_3 as seen, for example, in Eqs. (6.12) and (6.15). Additional amusing phenomenological points can be inferred from the above formulas. For example, at an e^+e^- collider, at large r the S_1 would be produced only via WW or $Z^* \to Z + S_1$, while S_2 and P_2 would be produced via $Z^* \to P_2 + S_2$. Note also that the couplings of S_2 and P_2 to down quarks are enhanced relative to the standard model, while their couplings to up quarks are suppressed, when $\tan\beta > 1$.

2. Limit of $x \gg v_1, v_2$ ($\lambda x, kx$ fixed)

As already discussed in Sec. III, this limit is such that S_1, S_2, and P_1 play the role of the two scalar and one pseudoscalar Higgs bosons of the minimal supersymmetry model. As expected, they have exactly the same couplings as found in Ref. 3 for the two scalar and one pseudoscalar Higgs bosons of the minimal supersymmetry model. On the other hand, S_3 and P_2 are completely decoupled and will not be detectable. The above remarks assume that it is the heavier pseudoscalar (P_2)

which is nearly pure $\text{Im}N$ in this limit, as discussed above Eq. (3.19). On the other hand, if the parameters should be such that the lighter pseudoscalar (P_1) is nearly pure $\text{Im}N$, then we must interchange the roles of P_1 and P_2; P_2 would play the role of the minimal model pseudoscalar and P_1 would decouple. All couplings involving a single P_2 would then turn out to have the opposite sign from the convention employed in Ref. 3, due to the fact that in this case $\gamma \rightarrow \pi/2$. However, this sign is purely a phase convention, and has no physical consequences.

3. Limit of $x \ll v_1, v_2$

Once again we use the explicit form of the Higgs-scalar mixing matrix appropriate to this case, Eq. (3.26), to compute the Higgs-boson couplings. We find the following results in the small-x limit:

$$R_{W^-C^+S_1}, R_{ZP_1S_1}$$

$$\sim \cos(\beta-\alpha)\left[1-\frac{4\lambda A_\lambda x \cos2\alpha \sin^2(\beta-\alpha)}{m_Z^2 \sin4\beta}\right],$$

$$(6.19)$$

$$R_{W^-C^+S_2}, R_{ZP_1S_2}$$

$$\sim -\sin(\beta-\alpha)\left[1+\frac{4\lambda A_\lambda x \cos2\alpha \cos^2(\beta-\alpha)}{m_Z^2 \sin4\beta}\right],$$

$$(6.20)$$

$$R_{W^-C^+S_3}, R_{ZP_1S_3} \sim \frac{2x \cot2\beta}{v}, \qquad (6.21)$$

and

$$R_{S_1W^+W^-}, R_{S_1ZZ}$$

$$\sim \sin(\beta-\alpha)\left[1+\frac{4\lambda A_\lambda x \cos2\alpha \cos^2(\beta-\alpha)}{m_Z^2 \sin4\beta}\right],$$

$$(6.22)$$

$$R_{S_2W^+W^-}, R_{S_2ZZ}$$

$$\sim \cos(\beta-\alpha)\left[1-\frac{4\lambda A_\lambda x \cos2\alpha \sin^2(\beta-\alpha)}{m_Z^2 \sin4\beta}\right],$$

$$(6.23)$$

$$R_{S_3W^+W^-}, R_{S_3ZZ} \sim \frac{-2x}{v}. \qquad (6.24)$$

As expected, we see that S_3 decouples in this limit, as does the P_2 state not appearing in the above formulas. They will be hard to produce and detect.

Of course, the above limiting cases are rather special and we shall see that typical results are often such that the vector-boson coupling strengths are shared among all the Higgs bosons, and that none of the latter are completely decoupled. For this purpose we must turn to a numerical study of the Higgs-boson couplings.

F. Numerical results for coupling constants

Among the above couplings it will be useful to present some results for those that are critical to Higgs-boson production at hadron or e^+e^- colliders. At a hadron collider, the two most important production modes are gluon fusion via a heavy-quark loop (sensitive to the $q\bar{q}$ couplings of the Higgs boson) and W^+W^- fusion to the Higgs boson (dependent upon the VV coupling). At an e^+e^- collider, $e^+e^- \rightarrow \bar{\nu}\nu + H$ via W^+W^- fusion and associated production via $e^+e^- \rightarrow Z^* \rightarrow Z + S$ will yield a usable cross section for a Higgs boson with sizable VV couplings, while pair-production modes such as $e^+e^- \rightarrow \gamma^* \rightarrow C^+C^-$ and $e^+e^- \rightarrow Z^* \rightarrow S+P$ must be used for the remaining Higgs bosons. Thus we first examine the VV couplings of the various neutral-scalar Higgs bosons, S_i. The magnitude of g_{VVS_i} relative to $g_{VVH_{SM}}$, defined as R_{VVS_i} in Eq. (6.9), is plotted as a function of m_C in Fig. 5(a) for some of the representative choices of $\tan\beta$, r, λ, and k considered for the mass plots given earlier. In particular, we focus on the two fixed-point value cases characterized by $\tan\beta=1.5$ and moderate r, $r=0.1$ and $r=1$. In analogy to previous plots related to these cases, at each m_C a maximum and minimum value for a given coupling is given as obtained by scanning over the values A_k consistent with Eq. (4.3).

We see that in the fixed-point cases the heaviest scalar Higgs boson S_3 tends to have VV couplings that are $\lesssim 20\%$ of the standard-model value. This implies its production cross section will be $\lesssim 4\%$ of the standard-model value at the same Higgs-boson mass, for any production mode requiring the VV coupling. Results for the lighter two scalar Higgs bosons are more dependent upon the charged-Higgs-boson mass (and hence exact scalar mass) and upon the precise k, r, and λ case considered. We see that it is possible for one of the two light scalars to have most of the VV coupling, but that they might also share relatively equally the VV coupling strength. It is clearly possible for the lightest scalar S_1 to be weakly coupled (unlike the minimal supersymmetry case), but this is not preferred for cases generated by the full renormalization-group analysis.

Turning to the quark couplings, we present results for the $u\bar{u}$ and $d\bar{d}$ couplings of both scalar and pseudoscalar Higgs bosons in Figs. 5(b) and 5(c). The values of $\tan\beta$, r, λ, and k are the same as those considered in Fig. 5(a). Clearly, there is a large amount of variation in the possible coupling strength relative to that found in the standard model. Generally speaking, every scalar Higgs boson is strongly coupled either to down quarks or to up quarks. However, it is the top-quark couplings which are most relevant in production via gg fusion at a hadron collider and in Higgs-boson decay. The figures show that it is possible to have substantial suppression in this coupling. Turning to the two pseudoscalars, we observe that $q\bar{q}$ couplings of P_2 are generally quite weak, while P_1 has roughly half the standard-model strength in the coupling squared. Only that pseudoscalar which is strongly coupled to quarks will have a substantial gg fusion cross section at a hadron collider.

In Fig. 5(d) we plot the value of R_{ZSP}, defined in Eq.

(6.9). A value of $R_{ZSP} \sim 1$ results in an $e^+e^- \rightarrow Z^*$ $\rightarrow S + P$ cross section of order 0.1 unit of $R_{pt} \equiv \sigma/\sigma_{pt}$, in the absence of phase-space suppression. We see that P_1 is likely to be strongly coupled to the Z and at least one of the scalars, whereas P_2 is generally weakly coupled for these moderate r values.

The dependence of these results on $\tan\beta$ is quite significant. Only the VV coupling is fairly independent of $\tan\beta$. In general, for increasing $\tan\beta$ values the $d\bar{d}$ couplings are greatly enhanced at the expense of the $u\bar{u}$ couplings and large changes in the ZSP couplings also occur.

As a further illustration of the relative coupling strengths, we present results for the explicit renormalization-group solution of Eqs. (5.14) and (5.15), i.e., with A_λ (and, hence, m_C) and A_k fixed at the precise values determined by the renormalization-group equation evolution. These appear in Table III. Note that the VV coupling is shared quite equally among the three Higgs

TABLE III. Coupling strengths, as defined in Eq. (6.9), for the renormalization-group solution specified in Eqs. (5.14) and (5.15), and already considered in Table II.

Channel	S_1	S_2	S_3	P_1	P_2
R_{VVS}	0.56	0.6	0.57		
$R_{u\bar{u}S,u\bar{u}P}$	0.35	0.42	0.97	0.12	0.48
$R_{d\bar{d}S,d\bar{d}P}$	1.45	1.36	−1.1	0.49	1.98
R_{ZP_1S}	0.1	0.09	0.2		
R_{ZP_2S}	0.42	0.36	0.8		

scalars, that all have somewhat suppressed couplings to $u\bar{u}$ and somewhat enhanced couplings to $d\bar{d}$, and that ZP_1S_i couplings are very weak. The P_1 would thus be very difficult to produce at a e^+e^- collider. In contrast, the light masses for all the S_i, combined with their hav-
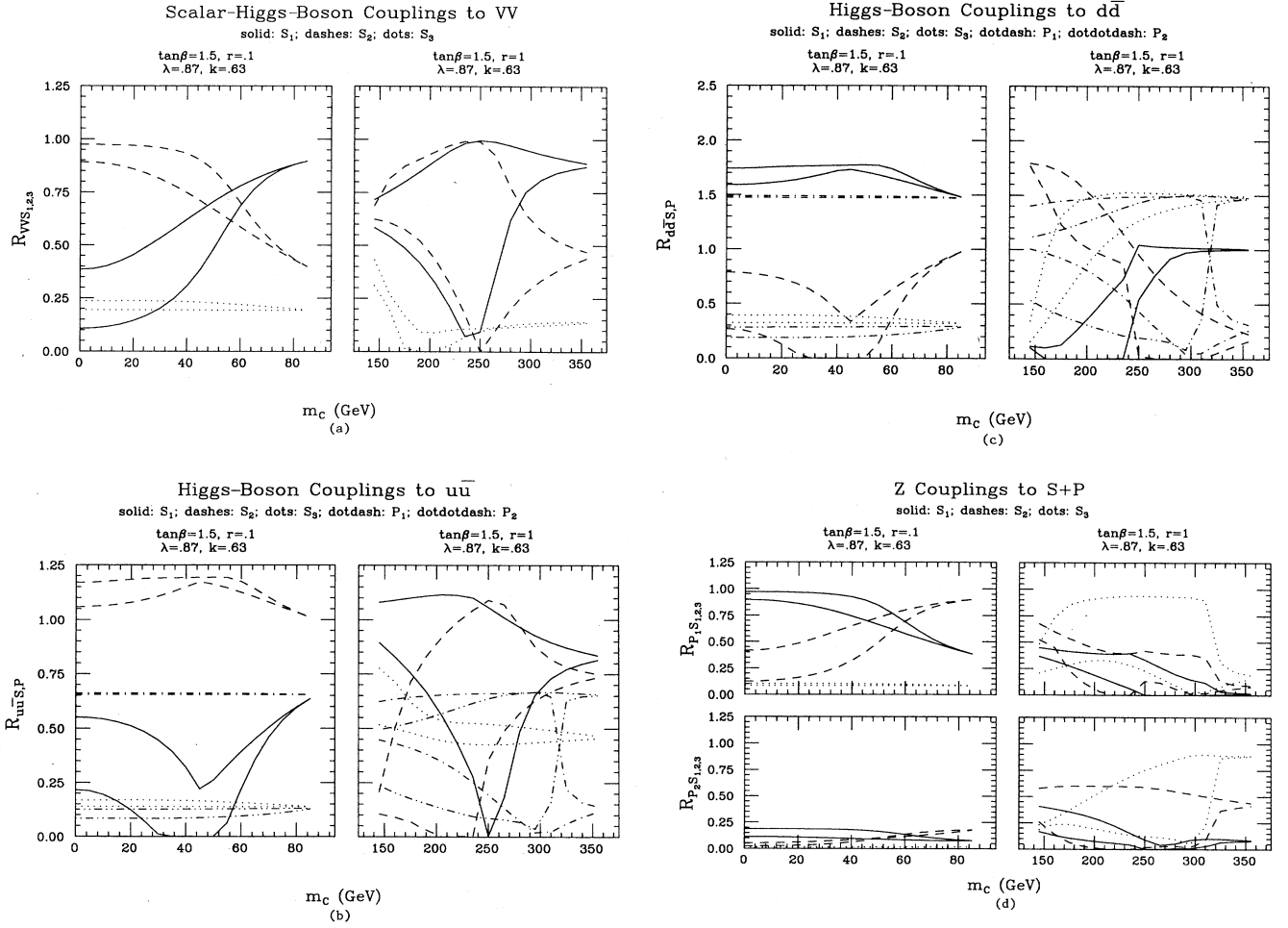

FIG. 5. The magnitude of the relevant S_i and P_i couplings, relative to the standard coupling strengths as defined in the text, as a function of m_C. The values $\lambda=0.87$, $k=0.63$, $\tan\beta=1.5$, and $r=0.1,1$ are considered. For each value of m_C, maximum and minimum values of the couplings are plotted, obtained by scanning over values of A_k which satisfy the constraints of Eq. (4.3). The following couplings are considered: (a) VVS_i couplings ($i=1,2,3$); (b) couplings to $u\bar{u}$; (c) couplings to $d\bar{d}$; (d) ZS_iP_j couplings ($i=1,2,3, j=1,2$).

ing at least $\frac{1}{4}$ the maximum possible VVS_i and $Z^* \to ZS_i$ squared couplings, imply large production cross sections in e^+e^- collisions. For S_1, S_2, and P_2 LEP and SLC would be appropriate machines. For instance, $Z \to S_1 l^+ l^-$ and $Z \to S_2 l^+ l^-$ decays are kinematically allowed and are proportional to the square of the ZZS_i coupling. As a result they would occur at roughly $\frac{1}{3}$ the SM rate. The small P_2 mass and large $S_i P_2 Z$ couplings also imply substantial branching ratios for the decay of a real Z to $S_1 P_2$ and $S_2 P_2$. The S_3 would be best produced via $e^+e^- \to Z^* \to ZS_3$; a new generation of e^+e^- colliders, with $\sqrt{s} \gtrsim 300$ GeV, would be most appropriate. At a hadron collider, real Z decays would be a significant source of $S_1 P_2$ and $S_2 P_2$ pairs. In addition, gg fusion would yield substantial inclusive cross sections for the S_1, S_2, and P_2, and be a primary production mode for S_3. Another possibly useful source of $S_{1,2,3}$ production would be via $W^* \to W S_{1,2,3}$. Regarding P_1, the absence of VV couplings and its weak coupling to $t\bar{t}$ imply that it is very weakly produced, just as in e^+e^- collisions. Obviously, the weak P_1 couplings are due to the fact that it has a large ImN component. We defer discussion of the charged Higgs boson and of the decays of the Higgs bosons for this special case to the following section.

To summarize, we have focused in this section on examples in which the value of r is moderate. Results at large $x \gg v_1, v_2$ are somewhat different, especially for the pseudoscalars. However, moderate to small r is strongly preferred by the renormalization group. We have seen that the larger parameter space of the present model, as compared to the minimal supersymmetric extension of the standard model, allows for greater structure in the Higgs-boson couplings. For example, the lightest scalar Higgs boson is not always the one with strongest VV couplings. Correspondingly, the cross sections for Higgs-boson production exhibit considerable variety. Generally, we find that some Higgs bosons will be very difficult to produce (in particular, either P_1 or P_2 tends to have a large ImN component and would be unobservable) while others will be relatively easy to make.

VII. HIGGS-BOSON DECAYS AND BRANCHING RATIOS

In the previous section, we have explored the couplings of the Higgs bosons of the theory to other Higgs bosons, vector bosons, and quarks. These are the couplings that are crucial for production of the Higgs bosons as already outlined. They also lead to important Higgs-boson decay modes to final states such as quark plus antiquark, vector boson plus lighter Higgs boson, a pair of vector bosons, and a pair of lighter Higgs bosons. However, in considering the decays of the Higgs bosons, we must also include the additional channels involving the supersymmetric states, in particular decay modes containing two neutralinos, a neutralino and a chargino, two charginos, or a pair of squarks or sleptons. The relevant couplings are easily obtained from the diagonalization procedures for the Higgs-boson, chargino, neutralino, squark, and slepton mass matrices that have already been discussed or re-

ferred to in previous sections. We will not give explicit expressions here; they may be found in Ref. 34, expressed in terms of the Higgs-boson, neutralino, and chargino eigenvectors. (Note that the neutralino and chargino mass matrices and states are identical in the E_6 case considered there and in the present case.)

However, there are several crucial points regarding these latter channels that will allow us to simplify our branching-ratio analysis. First, in the model considered in this paper, we have seen that squark masses are never less than ~ 100 GeV and more typically a factor of 2 or so higher. In contrast, there can be very light neutralinos and charginos, and even the heaviest neutralinos and charginos are lighter than the squarks. Thus, except for the heavier possible Higgs bosons in the fixed-point parameter cases investigated in Sec. III, squark decays are not allowed, whereas a significant number of neutralino-chargino channels are. Even for the heavy Higgs bosons with mass $\gtrsim 250$ GeV, for which squark channels might be allowed, the neutralino-chargino channels will be dominant. This same remark also applies for all Higgs-boson masses in comparing channels with a pair of sleptons (which can be relatively light in our model) to channels containing a pair of neutralinos or charginos. This is due to a feature of the squark-slepton versus chargino-neutralino couplings to Higgs bosons. The typical squark-squark coupling to a Higgs boson is proportional to gm_W or gm_Z leading to a partial decay width $\Gamma(H \to q\bar{q}) \sim g^2 m_W^2 / m_H$. In contrast, the fermion trace associated with Higgs-boson decay to a neutralino or chargino pair state brings in Higgs-boson-mass factors yielding a partial decay width $\Gamma(H \to \tilde{\chi}\tilde{\chi}) \sim g^2 m_H$. Thus the neutralino and chargino channels will have a natural enhancement factor of order m_H^2 / m_W^2 relative to squark and slepton final states. As a result, if both types of decays are kinematically allowed, and since the relevant m_H values are significantly above m_W, the Higgs-boson decays into squark and slepton pairs are not an important contribution to the total decay rate. This was illustrated in the case of the minimal supersymmetric model in Ref. 3. Thus we have dropped the squark and slepton channels from our analysis.

We will illustrate the range of possible Higgs branching ratios in the fixed-point cases of Eq. (5.2) with $\tan\beta = 1.5$ and $r = 0.1$ or $r = 1.0$, denoting them by their r values in what follows. We remind the reader that in each case we will present results obtained by varying over all A_k and m_C values that give an acceptable symmetry-breaking minimum. We have adopted a gluino mass of $m_{\tilde{g}} = 200$ GeV and a top mass of 70 GeV. Note that the value of $m_{\tilde{g}}$, in combination with the stated vacuum expectation value parameters and λ, k choices, completely fixes the chargino-neutralino mass matrix and couplings. This is because a choice for $m_{\tilde{g}}$ determines as well the SU(2)$_L$ and U(1) gaugino masses via the renormalization-group equations. We present our results in Fig. 6, which is divided into six parts, one for each of the Higgs bosons S_1, S_2, S_3, P_1, P_2, and C^+. In each part we have used the value of m_C to specify where in mass space (see Fig. 1) for a given Higgs boson we are. Each part contains

two windows corresponding to the two different cases outlined above. As in Fig. 1, at fixed m_C we have varied the remaining parameter A_k over the entire range allowed by the requirement of an acceptable local scalar

field minimum. Thus, for each channel plotted we give the maximum and minimum branching ratios, obtained in the course of the A_k scan, as a function of m_C. The channels considered are (1) the sum over all $q\bar{q}$ quark-
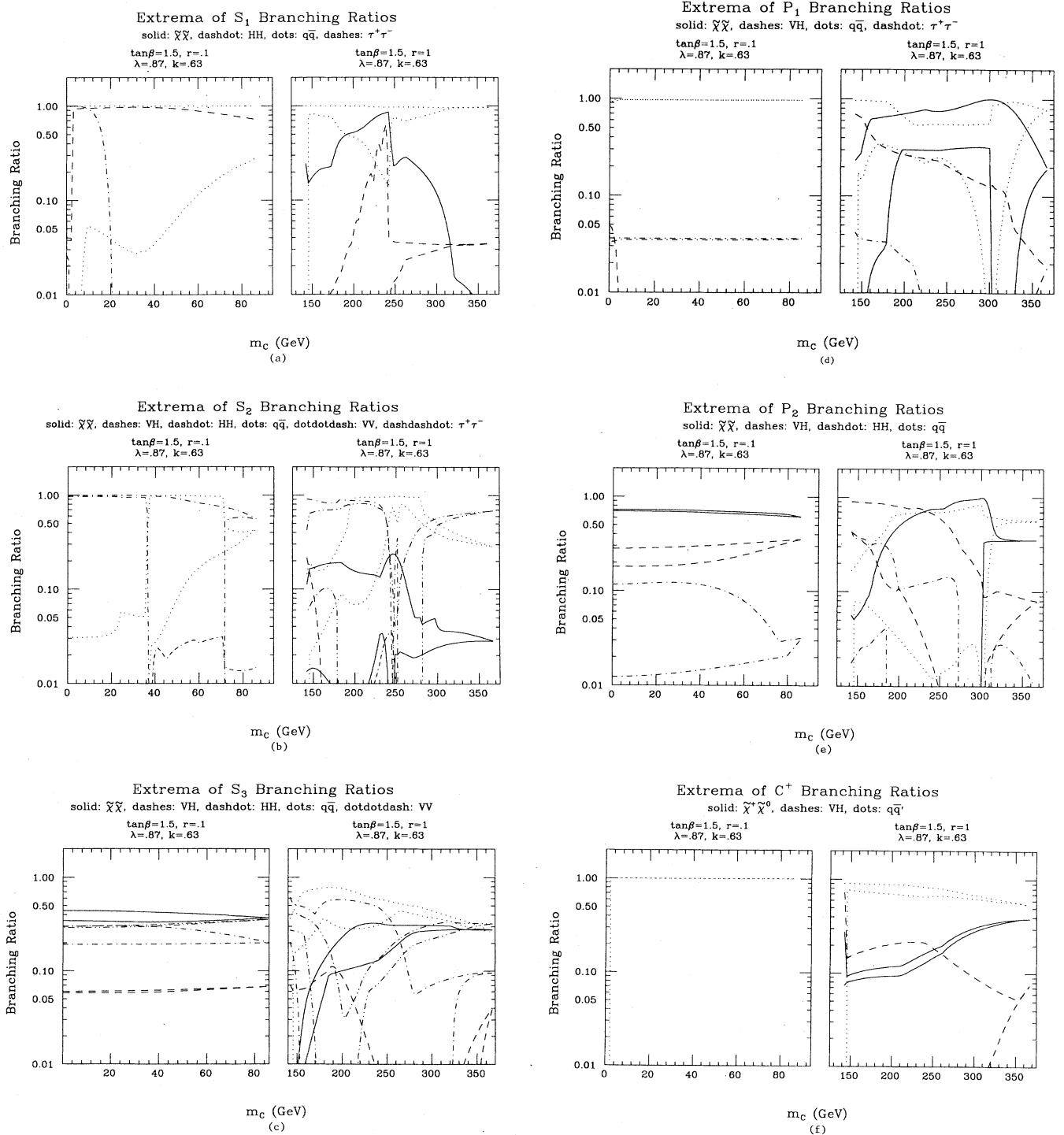

FIG. 6. The branching ratios for the different Higgs bosons as a function of m_C. At each m_C, maximum and minimum values of a given channel's branching ratio (as obtained by scanning over allowed A_k values) are given. See the text for a detailed description. The different plots are for (a) S_1, (b) S_2, (c) S_3, (d) P_1, (e) P_2, and (f) C^+.

antiquark pair channels—dominated, of course, by the heaviest allowed quark-antiquark pair, (2) the analogous sum over all $l\bar{l}$ lepton-antilepton pair channels, (3) the sum over all HH Higgs-boson pair channels, (4) the sum over all VH Higgs-boson plus vector-boson channels, (5) the sum over all VV vector-boson pair channels, and (6) the sum over all $\bar{\chi}\chi$ neutralino and chargino pair channels. Combined, these comprise the bulk of allowed decay modes. Fortunately, not all the above channels appear in the case of any one Higgs boson. Those that are present are indicated on a given figure along with the curve legend.

We will make a few general observations regarding the content of these figures in the case of each of the Higgs bosons.

S_1: For all choices of r, the S_1 can be very light, in which case its decays are dominated by $q\bar{q}$ and $l\bar{l}$ channels. The particular channel or combination of channels is determined by the precise value of m_{S_1}. For $m_{S_1} > 2m_b$ the $b\bar{b}$ channel is dominant, with $l\bar{l}$ being small. For $2m_b > m_{S_1} > 2m_c, 2m_\tau$ the $\tau^+\tau^-$ mode is dominant with the $c\bar{c}$ mode also significant but suppressed relative to standard-model expectations by mixing-angle factors. If $m_{S_1} < 2m_\tau$ the $s\bar{s}$ mode dominates; this possibility, however, is disfavored by our renormalization-group analysis. An exception to this dominance by $q\bar{q}$ and $l\bar{l}$ occurs for $r = 0.1$ when $m_{S_1} > 2m_C$ (recall that the charged-Higgs-boson mass can be very small in this case). When allowed, the $S_1 \rightarrow C^+C^-$ mode becomes dominant. At $r = 1$, neutralino-chargino modes may enter and in certain mass regions even be dominant.

S_2: In the $r = 0.1$ case we see that S_2 decays are dominated by $b\bar{b}$ or HH final states, with the latter being dominant when allowed. Regarding the latter, at low m_C ($\lesssim 40$ GeV) the C^+C^- mode is allowed and dominant. At higher m_C this mode is forbidden; but provided the A_k parameter is chosen so that m_{S_1} is small, $S_2 \rightarrow S_1 S_1$ will be the dominant decay. At $r = 1$, the decay possibilities are much more complex. We see that WW and ZZ decay modes can be very important for some A_k choices at a given m_C, but that at the same m_C it is also possible to choose A_k so that HH modes (mainly $S_1 S_1$ and, when kinematically allowed, $P_1 P_1$) are dominant. In addition, in the central region of m_C the S_2 mass drops below $2m_W$ and $b\bar{b}$ decays become very important. Finally, we see that neutralino-chargino decays (mainly $\bar{\chi}_1^+\bar{\chi}_1^-$) emerge as a significant component of the S_2 decays.

S_3: At $r = 0.1$ we are not far removed from the small x limit in which the S_3 tends to decouple from nonsinglet particles. However, there remains a large coupling to neutralinos and charginos. Thus the $\bar{\chi}\chi$ modes dominate with $\bar{\chi}_1^+\bar{\chi}_1^-$ being the most important component. We see that this channel is followed closely by VV and then HH. The HH modes are $P_1 P_1$, $S_1 S_1$, $S_1 S_2$, and C^+C^-. At a lower level we find VH decays where the latter is ZP_1 or $W^\pm C^\mp$ (in ratio 1:2). At $r = 1$, we see a large selection of modes, including $t\bar{t}$, HH, VV, and $\bar{\chi}\chi$, the latter two emerging mainly at higher m_C (and, hence, m_{S_3}) values.

P_1: At $r = 0.1$ only $b\bar{b}$ decays are important, or $\tau^+\tau^-$ where $b\bar{b}$ is forbidden at the lowest P_1 masses. At $r = 1$ we see that P_1 decays are dominated by a combination of $t\bar{t}$ and $\bar{\chi}\chi$ modes, although at low m_C the VH modes enter significantly.

P_2: At $r = 0.1$ we have a situation closely analogous to that for the S_3 at this same r value; the P_2 has suppressed couplings to all but the chargino-neutralino modes, which are dominant. Among these the $\bar{\chi}^+\bar{\chi}^-$ modes are the most important. The next most important channel is VH, including $W^\pm C^\mp$, ZS_1, and ZS_2. At a still lower level we find HH modes, dominated by $S_3 P_1$. At $r = 1$ $t\bar{t}$ and $\bar{\chi}\chi$ modes (largely $\bar{\chi}^+\bar{\chi}^-$) are dominant except at low m_C values where VH modes ($W^\pm C^\mp$ is often the largest, but ZS_1, ZS_2, and ZS_3 can be substantial also) become crucial.

C^+: At $r = 0.1$ only $c\bar{s}$ decays are important. At $r = 1$ the primary channel is $t\bar{b}$ with $\bar{\chi}^+\chi^0$ modes becoming significant at large m_C.

It is also useful to tabulate the predicted branching ratios for various channels in the representative renormalization-group solution, with parameters as detailed in Eqs. (5.14) and (5.15). In particular, for this table A_k and m_C (which determines A_λ) are fixed. The masses of all the particles for this particular renormalization-group solution were given in Table II. The couplings appeared in Table III. The branching ratios for a variety of interesting channels appear in Table IV. We see that among the neutral Higgs bosons, $b\bar{b}$ is the dominant mode except in the case of S_3 where HH modes are dominant. For the S_3, among the HH modes the $P_2 P_2$ mode is the largest with a branching ratio B of 0.38, followed by $S_1 S_1$ with $B \sim 0.19$. The S_3 also has some $\bar{\chi}\chi$ decays, with total $B \sim 0.05$. None of the neutral Higgs bosons are heavy enough to have any VH or VV decays. In the case of the C^+, its mass is too small to allow the $t\bar{b}$ mode, and, as a result, its decays are dominated by $\bar{\chi}_1^+\chi_1^0$.

Let us briefly consider prospects for detecting the Higgs bosons in the special renormalization-group case, given the branching ratios described in the previous paragraph and the production cross sections outlined in the previous section. Consider first e^+e^- collisions. Detection of the $S_{1,2}$ Higgs bosons at an e^+e^- collider would be straightforward,[35] either in $Z \rightarrow S_{1,2} l^+ l^-$ decays or $Z \rightarrow S_{1,2} P_2$ decays. In the latter case, one would search in final states containing two $b\bar{b}$ pairs; backgrounds would probably not be a problem. S_3 production via

TABLE IV. Branching ratios of the various Higgs bosons to a variety of interesting channels, for the special renormalization-group solution of Eqs. (5.14) and (5.15). See Tables II and III for the masses and couplings of the states involved.

Channel	S_1	S_2	S_3	P_1	P_2	C^+
$q\bar{q}$	0.92	0.81	0.13	0.96	0.96	0.01
$l\bar{l}$	0.08	0.03	0.005	0.04	0.04	0.006
HH	0	0.16	0.82	0	0	0
$\bar{\chi}\chi$	0	0	0.05	0	0	0.99

$Z^* \rightarrow S_3 Z$ would require a $\sqrt{s} \gtrsim 300$ GeV machine;[36] the dominance of $S_3 \rightarrow HH$ modes would lead to $Zb\bar{b}b\bar{b}$ final states, which would probably be detectable. P_1 is essentially hopeless because of its small production rate. Detection of the charged Higgs boson would also not be straightforward. Even though the $\gamma^* \rightarrow C^+ C^-$ cross section at a $e^+ e^-$ collider with $\sqrt{s} \gtrsim 300$ GeV (Refs. 36 and 37) would be of order $\frac{1}{4}$ unit of R_{pt}, the $\bar{\chi}_1^+ \bar{\chi}_1^0$ decays for both the produced charged Higgs bosons would make direct mass reconstruction impossible (the $\bar{\chi}_1^0$ would be the LSP). Turning to a hadron collider, we first consider detection of $Z \rightarrow S_{1,2} P_2$ events. Unfortunately, the $b\bar{b}b\bar{b}$ final states would presumably have large QCD backgrounds, so that discovery in this mode might prove difficult. A detailed study is required. The S_3 scalar Higgs boson definitely falls into the category of "intermediate mass" approaches.[38] Its mass is such that only the production-detection mode of $W^* \rightarrow W (\rightarrow l\nu) S (\rightarrow b\bar{b})$ could be employed.[39] While current studies[40] of this mode have yielded optimistic results for a Higgs scalar with a mass above m_Z and with full standard-model VV couplings, it is likely that the reduction in cross section by a factor of $\sim 3-4$ for the S_3, combined with its mass being near that of the Z, will make this Higgs boson more difficult. The P_1, which has no VV couplings and is weakly coupled to quarks, will be essentially impossible to observe at a hadron collider. The most useful charged-Higgs-boson production mode would be $g\bar{b} \rightarrow C^+ \bar{t}$, followed by a trigger on the spectator $\bar{t}$ quark.[41] The $\bar{\chi}_1^+ \bar{\chi}_1^0$ decay might provide a sufficiently clean missing energy trigger to allow detection; a detailed study is needed.

In summary, Higgs-boson decays in this theory are complex and many channels must be examined before one can be certain of discovering or excluding a Higgs boson of any given type in any given mass range. In addition, even though the generally expected Higgs-boson masses are fairly modest, the most useful production cross sections are often not as large as in the corresponding standard-model Higgs-boson case. The most uniform example of this latter statement occurs at small r, where the S_3 and P_2 tend to decouple from nonsinglet particles including the standard model quarks and gauge bosons. Thus, we typically find that one or more of the Higgs bosons will be difficult to detect at both an $e^+ e^-$ collider and a hadron collider.

VIII. CONCLUSIONS

We have argued that a supersymmetric model in which a singlet Higgs field is present, in addition to the two Higgs-doublet fields that are absolutely required, provides an attractive solution to the μ-parameter naturalness problem of the minimal supersymmetric model. We have also noted that such a singlet field is present in most superstring models with low-energy $N = 1$ supersymmetry, including the attractive SU(5)$\times$U(1) four-dimensional superstring model.[7] We have then proceeded to explore the implications of such a theory for the Higgs-boson sector, assuming that only trilinear couplings enter into the superpotential (as is automatically the case in the simpler superstring approaches). The

physical Higgs bosons of the theory comprise three scalars (S_1, S_2, and S_3), two pseudoscalars (P_1 and P_2), and a charged Higgs pair ($C^{\pm}$). While there are, in principle, a number of parameters that need to be specified in order to determine the theory, we have found that the renormalization-group and grand unification constraints impose surprisingly stringent restrictions on the allowed range of these parameters, especially if the entire source of supersymmetry breaking at the grand unification mass scale M_X is from a common gaugino mass, M_U (Ref. 23). The resulting phenomenology for the Higgs bosons is complex, but with many regularities. For instance, as in earlier investigations of other $N = 1$ supersymmetric models,[1,3,14,15] we find that there is always a light scalar Higgs boson with mass $\lesssim 150$ GeV. The introduction of the singlet field allows us to have charged-Higgs-boson masses lighter than m_W (unlike earlier models) but the corresponding parameter choices are not preferred by the renormalization-group analysis. In general, several of the other Higgs bosons will be fairly heavy, but always below 1 TeV in mass except in extreme cases. Despite the generally modest mass scale for the Higgs bosons, we have seen that detection of all of them will represent a formidable challenge—production cross sections can be small and decays can be complex or subject to large backgrounds.

For the allowed renormalization-group solutions where supersymmetry is broken only by the gaugino mass M_U at M_X, we have solved for the masses of all physical particles. The constraint imposed by requiring that the vacuum structure be that observed in nature (i.e., no charge or color breaking, but standard electroweak symmetry breaking) is very powerful indeed. Only a very narrow range of choices for the basic trilinear couplings of the superpotential yield allowed solutions. The predicted range of masses of all the physical particles is very small, and appears in Table I. We find a top-quark mass between 75 and 93 GeV, a gluino mass between 140 and 260 GeV, and light charginos, sleptons, and sneutrinos. In addition, all Higgs bosons have mass below 100 GeV, with the lightest scalar certainly accessible at LEP and SLC. Indeed, if there is any truth to this general approach the next few years should provide an abundance of new and exciting physics, in particular allowing our first experimental probes of the Higgs-boson sector that is at the basis of electroweak symmetry breaking. However, in exploring the Higgs-boson sector, we have seen that it will be necessary to consider a variety of different decay channels, with, in particular, channels containing lighter Higgs-boson pairs, a vector boson plus a lighter Higgs boson, or neutralino-chargino pairs. The resulting final states should all be explored more thoroughly with regard to important backgrounds and experimental cuts. Overall, this study makes explicit the fact that we must not rely on studies conducted purely in the context of the standard model in assessing the ability of new colliders and detectors to study the Higgs sector.

APPENDIX A: POTENTIAL INCLUDING TOP AND BOTTOM SQUARK DEGREES OF FREEDOM

In this appendix we give the full scalar field potential, after including top (both left and right) and bottom (left only) squark fields through the superpotential coupling hQU^cH_2 and the associated soft supersymmetry-breaking terms. We have made the approximation that all the colored fields are parallel in color space. We shall discuss later the justification for this approximation and describe the generalizations that would be required to include full color degrees of freedom.

We begin by listing the simplifications that may be made by employing the gauge and phase degrees of freedom of the scalar fields. Our notation for the squark scalar fields is $\widetilde{Q}$ for the top-bottom doublet ($\widetilde{U},\widetilde{D}$), and $\widetilde{U}^c$ for the top squark singlet field.

(1) $SU(2)_L$ transformations may be used to set $v^+=0$.

(2) The phase of the N field may be chosen so that $kA_k \in \mathbf{R}^+$.

(3) The phase of H_1 can be chosen so that $\lambda A_\lambda \in \mathbf{R}^+$.

(4) The phase of $\widetilde{U}^c$ can be chosen so that $hA_h \in \mathbf{R}^+$.

(5) The phase of H_2 can be chosen so that $v_2 \in \mathbf{R}^+$.

(6) The phase of $\widetilde{Q}$ can be chosen so that $u \equiv \langle \widetilde{U} \rangle \in \mathbf{R}^+$.

(7) Finally, it turns out that the above conventions imply that the phases of v^- and $d \equiv \langle \widetilde{D} \rangle$ enter only in the combination $v^{-*}d$, so that we may choose $d \in \mathbf{R}^+$.

The most general form for the vacuum expectation value of the resulting potential is given below.

$$\langle V_D^{U(1)} \rangle = \frac{g'^2}{8}(-|v_1|^2-|v^-|^2+v_2^2+\tfrac{1}{3}u^2+\tfrac{1}{3}d^2-\tfrac{4}{3}|u^c|^2)^2 \ ,$$

$$\langle V_D^{SU(2)} \rangle = \frac{g^2}{8}[(|v_1|^2+|v^-|^2+v_2^2+u^2+d^2)^2-4(|v_1|^2v_2^2+|v_1|^2d^2+v_2^2u^2+|v^-|^2u^2)+4ud(v_1^*v^-+v_1v^{-*})] \ , \qquad (A1)$$

$$\langle V_D^{SU(3)} \rangle = \frac{g_s^2}{6}(u^2+d^2-|u^c|^2)^2 \ ,$$

$$\langle V_F \rangle = \lambda^2[(|v_1|^2+|x|^2)v_2^2+(|v_1|^2+|v^-|^2)|x|^2]+h^2[(u^2+d^2)|u^c|^2+(|u^c|^2+u^2)v_2^2]$$

$$+k^2|x|^4-\lambda k v_2(v_1x^{*2}+v_1^*x^2)-\lambda h[u(v_1xu^{c*}+v_1^*x^*u^c)+d(v^-xu^{c*}+v^{-*}x^*u^c)] \ , \qquad (A2)$$

$$\langle V_{\text{soft}} \rangle = m_{H_1}^2(|v_1|^2+|v^-|^2)+m_{H_2}^2v_2^2+m_N^2|x|^2+m_{\widetilde{Q}}^2(u^2+d^2)+m_{\widetilde{U}^c}^2|u^c|^2-\lambda A_\lambda(v_1x+v_1x^*)v_2$$

$$-\frac{kA_k}{3}(x^3+x^{*3})-hA_hv_2u(u^c+u^{c*}) \ , \qquad (A3)$$

where we have taken λ,k,h relatively real in order to avoid explicit CP breaking. This does not, however, guarantee that there is no spontaneous breaking of CP. If $u,d \neq 0$ then there is no choice for the signs of λk and λh that guarantees that the potential minimum occurs when all fields have zero phase; the phase-dependent term in $\langle V_D^{SU(2)} \rangle$ enters with the wrong sign in comparison to all the other phase-dependent terms which would be minimized for zero phase if $\lambda k, \lambda h \in \mathbf{R}^+$. However, we shall only explore color breaking for $\lambda k, \lambda h \in \mathbf{R}^+$, since we are only interested in assessing whether minima of the pure Higgs potential, found subject to this constraint, are true global minima.

As stated earlier, the above potential has been written in the approximation that all the colored fields (u, d, and u^c) are parallel in color space. We will not explore the complete color space degrees of freedom because of the greatly increased complexity of analysis that would result. We argue that this is a good approximation when u, d, and u^c are of the same order as v_1,v_2,x. Since g_s is much larger than λ or k for the solutions that we have obtained using the unification boundary conditions of Eq. (5.1), the largest single term in the potential is $\langle V_D^{SU(3)} \rangle$. An examination of the full color structure of this term reveals that it is minimized for configuration in which u, d, and u^c are all parallel in color space. More generally, however, we must regard any restrictions that we discover on our potential parameters, through requiring the $u,d,u^c=0$ at the global minimum, as being necessary but not clearly sufficient.

The procedure followed as part of the renormalization-group investigation of Sec. V was the following. Given a set of parameters obtained by evolving from the grand unification scale M_X down to M_{SUSY}, beginning with initial choices for λ_U, k_U, and h_U and the boundary condition (5.1), we required that the resulting low-energy parameters yield a global minimum of the complete potential such that all the neutral Higgs fields, and *only* the neutral Higgs fields, acquire nonzero vacuum expectation values. This required examining not just the Higgs potential, but rather the complete scalar field potential as delineated above, including the colored fields

$\tilde{Q}$ and $\tilde{U}^c$. Overall there are 11 degrees of freedom after making use of all independent phase rotations and $SU(2)_L \times U(1)_Y$ gauge transformations. They are v_1, v_1^*, v_2, x, x^*, v^-, v^{-*}, u, d, u^c, and u^{c*}, where $u = \langle \tilde{U} \rangle$, $d = \langle \tilde{D} \rangle$, $u^c = \langle \tilde{U}^c \rangle$. As noted above, u and d can be taken to be real, but the potential form is such that there is no simple set of choices for the relative signs of the potential parameters which guarantees that the other VEV's are real. (Only in the subspace where either d or v^- is zero is this possible. This contrasts with the case where the colored field VEV's are ignored.) Thus, for a given set of low-energy parameters, we have numerically searched the 11-dimensional VEV space for all local minima of the full potential, and determined which is the global minimum. If the global minimum is not of the desired type we discard the solution.

Our procedure in practice was to first consider the scalar potential without including colored degrees of freedom. We then searched for solutions starting from the boundary conditions (5.1) such that at the potential minimum the requirements of Eq. (5.5) were met and charge breaking ($v^- \neq 0$) was not present. Once such a solution was obtained we then turned to the full scalar potential, including colored degrees of freedom as specified above, and determined whether there was a color breaking (u, d, or $u^c \neq 0$) minimum of still lower energy. We found that this never occurred, i.e., the requirements of Eq. (5.5) and $v^- = 0$ for the scalar potential without colored fields already selected solutions that did not break color once the colored degrees of freedom were included. This is the case because the values of $m_{\tilde{Q}}^2$ and $m_{\tilde{U}^c}^2$ generated by the renormalization-group equations are quite substantial in comparison to the other mass parameters of the low-energy potential. As a result, nonzero values of the colored field VEV's are disfavored. Of course, if we choose to ignore the results of the renormalization-group equations and allow $m_{\tilde{Q}}^2$, $m_{\tilde{U}^c}^2$, and A_h to take on arbitrary values, then color-breaking minima can result, as we saw in Sec. IV.

APPENDIX B: TRILINEAR HIGGS SELF-COUPLINGS

In this appendix, we summarize results for the trilinear Higgs self-couplings using the Π symbols defined in Eq. (6.8). The results are

$$-g_{S_a P_\beta P_\gamma} = \frac{\bar{g}^2}{2\sqrt{2}}[(\Pi_{a\beta\gamma}^{222} - \Pi_{a\beta\gamma}^{211})v_2 + (\Pi_{a\beta\gamma}^{111} - \Pi_{a\beta\gamma}^{122})v_1] + \frac{\lambda A_\lambda}{\sqrt{2}}(\Pi_{a\beta\gamma}^{321} + \Pi_{a\beta\gamma}^{231} + \Pi_{a\beta\gamma}^{213}) + \frac{k A_k}{\sqrt{2}}\Pi_{a\beta\gamma}^{333}$$

$$+ \frac{\lambda^2}{\sqrt{2}}[(\Pi_{a\beta\gamma}^{322} + \Pi_{a\beta\gamma}^{311})x + (\Pi_{a\beta\gamma}^{233} + \Pi_{a\beta\gamma}^{211})v_2 + (\Pi_{a\beta\gamma}^{133} + \Pi_{a\beta\gamma}^{122})v_1]$$

$$+ \lambda k \sqrt{2}[(\Pi_{a\beta\gamma}^{321} - \Pi_{a\beta\gamma}^{123} - \Pi_{a\beta\gamma}^{231})x + (\tfrac{1}{2}\Pi_{a\beta\gamma}^{133} - \Pi_{a\beta\gamma}^{331})v_2 + (\tfrac{1}{2}\Pi_{a\beta\gamma}^{233} - \Pi_{a\beta\gamma}^{332})v_1] + k^2\sqrt{2}\Pi_{a\beta\gamma}^{333} \ . \tag{B1}$$

$$-g_{S_a S_b S_c} = \frac{\bar{g}^2}{2\sqrt{2}}[(\Pi_{abc}^{222} - \Pi_{abc}^{211})v_2 + (\Pi_{abc}^{111} - \Pi_{abc}^{122})v_1] - \frac{\lambda A_\lambda}{\sqrt{2}}(\Pi_{abc}^{321} + \Pi_{abc}^{333}) + k^2\sqrt{2}\Pi_{abc}^{333}x$$

$$+ \frac{\lambda^2}{\sqrt{2}}[(\Pi_{abc}^{233} + \Pi_{abc}^{211})v_2 + (\Pi_{abc}^{133} + \Pi_{abc}^{122})v_1 + (\Pi_{abc}^{322} + \Pi_{abc}^{311})x] + \lambda k \sqrt{2}(-\tfrac{1}{2}\Pi_{abc}^{332}v_1 - \tfrac{1}{2}\Pi_{abc}^{311}v_2 - \Pi_{abc}^{321}x) \ . \tag{B2}$$

$$-g_{S_a C^+ C^-} = \frac{g'^2}{4\sqrt{2}}[(\Pi_{a+-}^{222} - \Pi_{a+-}^{211})v_2 + (\Pi_{a+-}^{111} - \Pi_{a+-}^{122})v_1]$$

$$+ \frac{g^2}{4\sqrt{2}}[(\Pi_{a+-}^{222} + \Pi_{a+-}^{211} + \Pi_{a+-}^{121} + \Pi_{a+-}^{112})v_2 + (\Pi_{a+-}^{111} + \Pi_{a+-}^{122} + \Pi_{a+-}^{221} + \Pi_{a+-}^{212})v_1]$$

$$+ \frac{\lambda A_\lambda}{2\sqrt{2}}(\Pi_{a+-}^{312} + \Pi_{a+-}^{321}) + \lambda k \sqrt{2}\Pi_{a+-}^{312} + \frac{\lambda^2}{\sqrt{2}}[(\Pi_{a+-}^{322} + \Pi_{a+-}^{311})x - \Pi_{a+-}^{121}v_2 - \Pi_{a+-}^{212}v_1] \ . \tag{B3}$$

---

*Present address: CERN, Geneva, Switzerland.

†Present address: Warsaw University, Warsaw, Poland.

‡Also at Istituto Nazionale di Fisica Nucleare, Sezione di Padova, Italy.

[1] H. P. Nilles, Phys. Rep. 110, 1 (1984); H. E. Haber and G. L. Kane, ibid. 117, 75 (1985); A. B. Lahanas and D. V. Nanopoulos, ibid. 145, 1 (1987).

[2] In our conventions, H_1 is the Higgs boson coupled to charged leptons and down-type quarks, H_2 the Higgs boson coupled to up-type quarks.

[3] J. F. Gunion and H. E. Haber, Nucl. Phys. B272, 1 (1986); B278, 449 (1986); B307, 445 (1988).

[4] P. Fayet, Nucl. Phys. B90, 104 (1975); R. K. Kaul and P. Ma-

jumdar, ibid. B199, 36 (1982); R. Barbieri, S. Ferrara, and C. A. Savoy, Phys. Lett. 119B, 343 (1982); H. P. Nilles, M. Srednicki, and D. Wyler, ibid. 120B, 346 (1983); J. M. Frère, D. R. T. Jones, and S. Raby, Nucl. Phys. B222, 11 (1983); J. P. Derendinger and C. A. Savoy, ibid. B237, 307 (1984).

[5] As we will see in Sec. II, in order to avoid an axion there must also be other terms in W, such as $(k/3)N^3$.

[6] See, e.g., F. Zwirner, Int. J. Mod. Phys. A3, 49 (1988), and references therein.

[7] I. Antoniadis, J. Ellis, J. S. Hagelin, and D. V. Nanopoulos, Phys. Lett. B 194, 231 (1987); Report No. CERN-TH.4931/87 (unpublished); Report No. CERN-TH.5005/88 (unpublished); J. Ellis, J. S. Hagelin, S. Kelley, and D. V. Nanopoulos, Phys.

Lett. B **209**, 283 (1988).

[8]J. E. Kim and H. P. Nilles, Phys. Lett. **138B**, 150 (1984).

[9]L. Hall, J. Lykken, and S. Weinberg, Phys. Rev. D **27**, 2359 (1983).

[10]G. F. Giudice and A. Masiero, Phys. Lett. B **206**, 480 (1988).

[11]J. Polchinski and L. Susskind, Phys. Rev. D **26**, 3661 (1982); H. P. Nilles, M. Srednicki, and D. Wyler, Phys. Lett. **124B**, 337 (1983); A. B. Lahanas, *ibid.* **124B**, 341 (1983); L. Alvarez-Gaume, J. Polchinski, and M. B. Wise, Nucl. Phys. **B211**, 495 (1983).

[12]J. Ellis, K. Enqvist, D. V. Nanopoulos, K. Olive, M. Quirós, and F. Zwirner, Phys. Lett. B **176**, 403 (1986).

[13]K. Inoue, A. Kakuto, H. Komatsu, and S. Takeshita, Prog. Theor. Phys. **68**, 927 (1982); J. P. Derendinger and C. A. Savoy, Nucl. Phys. **B237**, 307 (1984); B. Gato, J. Lean, J. Perez-Mercader, and M. Quiros, *ibid.* **B253**, 285 (1985); N. K. Falck, Z. Phys. C **30**, 247 (1986).

[14]H. E. Haber and M. Sher, Phys. Rev. D **35**, 2206 (1987).

[15]J. Ellis, D. V. Nanopoulos, S. T. Petcov, and F. Zwirner, Nucl. Phys. **B283**, 93 (1987); J. F. Gunion, L. Roszkowski, and H. E. Haber, Phys. Lett. B **189**, 409 (1987); M. Drees, Phys. Rev. D **35**, 2910 (1987).

[16]If the pseudoscalar with mass $3kx A_k$ is the lighter of the two pseudoscalars, then $\gamma \rightarrow \pi/2$, and we must interchange $P_1 \leftrightarrow P_2$ in the following discussion.

[17]Technically, one might also require that this zero-field configuration should *not* be a local minimum of the potential, entailing that at least one of the soft mass-squared terms in the potential of Eq. (2.6) be negative. This condition would be imposed in order to avoid any possibility that the hot universe, originally in the symmetric vacuum, would be trapped in this metastable state at a temperature below that of the phase transition to the asymmetric vacuum. This is a somewhat model-dependent scenario, and we have not imposed such a condition on our parameters. However, we have checked that imposing this condition on the model-independent analysis of this section leads to very minor changes—the bounds on the Higgs-boson masses are slightly more restrictive in a very narrow range of parameter space when r is large. The renormalization-group analysis of Sec. V (which favors small r) is completely unaffected.

[18]However, this has not yet been proven as a theorem.

[19]S. Coleman and E. Weinberg, Phys. Rev. D **7**, 1888 (1973).

[20]J. P. Derendinger and C. A. Savoy, Nucl. Phys. **B237**, 307 (1984); L. E. Ibanez and J. Mas, *ibid.* **B286**, 107 (1987).

[21]J. F. Gunion, H. E. Haber, and M. Sher, Nucl. Phys. **B306**, 1 (1988).

[22]Since M_{SUSY} is in general not much larger than m_W, the reader might wonder why we introduce this new threshold. The reason is that, if one uses naively the supersymmetric renormalization-group equations, some of the parameters (e.g., $m_{H_2}^2$) have very large variations between M_{SUSY} and m_W, making such an approximation unreliable.

[23]P. Binetruy, S. Dawson, and I. Hinchliffe, Phys. Lett. B **179**, 262 (1986); J. Ellis, D. V. Nanopoulos, M. Quirós, and F. Zwirner, *ibid.* **180**, 83 (1986); J. Ellis, A. B. Lahanas, D. V. Nanopoulos, M. Quirós, and F. Zwirner, *ibid.* **188**, 408 (1987); P. Majumdar, Mod. Phys. Lett. **A2**, 49 (1987); P. Binetruy, S. Dawson, I. Hinchliffe, and M. K. Gaillard, Phys. Lett. B **192**, 377 (1987).

[24]Note that the assumptions $m_U \neq 0$, $M_U = A_U = 0$ and $A_U \neq 0$, $m_U = M_U = 0$ would not correspond to phenomenologically acceptable scenarios.

[25]S. L. Wu, in *Lepton and Photon Interactions,* Proceedings of the 1987 International Symposium on Lepton and Photon Interactions at High Energies, Hamburg, West Germany, 1987, edited by W. Bartel and R. Rückl [Nucl. Phys. B, Proc. Suppl. **3**, 39 (1987)].

[26]UA1 Collaboration, G. Arnison *et al.*, Europhys. Lett. **1**, 327 (1986).

[27]ASP Collaboration, C. Hearty *et al.*, Phys. Rev. Lett. **58**, 1711 (1987).

[28]UA1 Collaboration, C. Albajar *et al.*, Phys. Lett. B **198**, 261 (1987).

[29]J. Ellis, K. Enqvist, D. V. Nanopoulos, and F. Zwirner, Mod. Phys. Lett. **A1**, 57 (1986); R. Barbieri and G. F. Giudice, Nucl. Phys. **B306**, 63 (1988).

[30]UA1 Collaboration, C. Albajar *et al.*, Z. Phys. C **37**, 505 (1988).

[31]U. Amaldi *et al.*, Phys. Rev. D **36**, 1385 (1987); G. Costa *et al.*, Nucl. Phys. **B297**, 244 (1988); J. Ellis and G. Fogli, Phys. Lett. B **213**, 526 (1988).

[32]This is related to the fact that our solutions turn out to have $\tan\beta > 1.4$. For $\tan\beta$ strictly equal to 1, $m_{S_1} = 0$ since the determinant of the scalar mass matrix is zero in that case.

[33]M. Narain *et al.*, contributed paper to the 24th International Conference on High Energy Physics, Munich, August, 1988.

[34]J. F. Gunion, H. E. Haber, and L. Roszkowski, Phys. Rev. D **38**, 105 (1988).

[35]Convenient references for detection of a light Higgs boson at an e^+e^- machine are *Physics at LEP,* LEP Jamboree, Geneva, Switzerland, 1985, edited by J. Ellis and R. Peccei (CERN Report No. 86-02, Geneva, 1986); *Proceedings of the 2nd Mark II Workshop on SLC Physics,* Granlibakken, 1986, edited by K. Krieger (SLAC Report No. 306, Granlibakken, 1986).

[36]Studies of physics at high-energy e^+e^- colliders have been surveyed in C. Ahn *et al.* (SLAC Report No. 329, 1988) (unpublished); *Proceedings of the Workshop on Physics at Future Accelerators,* La Thuile, Italy, 1987, edited by J. H. Mulvey (CERN Report No. 87-07, Geneva, Switzerland, 1987).

[37]A study of charged-Higgs-boson detection in quark decay modes appears in S. Komamiya, Phys. Rev. B **38**, 2158 (1988).

[38]See J. F. Gunion, G. L. Kane, and J. Wudka, Nucl. Phys. **B299**, 231 (1988) for a survey.

[39]J. F. Gunion, P. Kalyniak, M. Soldate, and P. Galison, Phys. Rev. D **34**, 101 (1986); Phys. Rev. Lett. **54**, 1226 (1985).

[40]D. Atwood, J. Brau, J. Gunion, G. Kane, R. Madaras, D. Miller, L. Price, and L. Spadafora, in *Experiments, Detectors, and Experimental Areas for the Supercollider,* proceedings of the Workshop, Berkeley, California, 1987, edited by R. Donaldson and M. Gilchriese (World Scientific, Singapore, 1987), p. 728.

[41]J. F. Gunion, H. E. Haber, F. E. Paige, W. Tung, and S. S. D. Willenbrock, Nucl. Phys. **B294**, 621 (1987); J. F. Gunion, H. E. Haber, S. Komamiya, H. Yamamoto, and A. Barbaro-Galtieri, *Experiments, Detectors, and Experimental Areas for the Supercollider,* edited by R. Donaldson and M. Gilchriese (World Scientific, Singapore, 1987), p. 110.